Exercise-derived peptide protects against pathological cardiac remodeling

Anwen Yin,[a,1] Ruosen Yuan,[a,1] Qingqing Xiao,[a] Weifeng Zhang,[a] Ke Xu,[a] Xiaoxiao Yang,[a] Wentao Yang,[a] Lei Xu,[a] Xia Wang,[a] Fei Zhuang,[a] Yi Li,[a] Zhaohua Cai,[a] Zhe Sun,[c] Bin Zhou,[b] Ben He,[a]* and Linghong Shen[a]*

[a]Department of Cardiology, Shanghai Chest Hospital, Shanghai Jiao Tong University School of Medicine, Shanghai 200030, China
[b]Chinese Academy of Sciences, University of Chinese Academy of Sciences, Shanghai, China
[c]School of Life Science and Technology, Shanghai Tech University, Shanghai, China

eBioMedicine 2022;82: 104164
Published online xxx
https://doi.org/10.1016/j.ebiom.2022.104164

Summary

Background Exercise training protects the heart against pathological cardiac remodeling and confers cardioprotection from heart failure. However, the underlying mechanism is still elusive.

Methods An integrative analysis of multi-omics data of the skeletal muscle in response to exercise is performed to search for potential exerkine. Then, CCDC80tide is examined in humans after acute exercise. The role of CCDC80tide is assessed in a mouse model of hypertensive cardiac remodeling and in hypertension-mediated cell injury models. The transcriptomic analysis and immunoprecipitation assay are conducted to explore the mechanism.

Findings The coiled-coil domain-containing protein 80 (CCDC80) is found strongly positively associated with exercise. Interestingly, exercise stimuli induce the secretion of C-terminal CCDC80 (referred as CCDC80tide hereafter) via EVs-encapsulated CCDC80tide into the circulation. Importantly, cardiac-specific expression of CCDC80tide protects against angiotensin II (Ang II)-induced cardiac hypertrophy and fibrosis in mice. In *in vitro* studies, the expression of CCDC80tide reduces Ang II-induced cardiomyocyte hypertrophy, cardiac microvascular endothelial cell (CMEC) inflammation, and mitigated vascular smooth muscle cell (VSMC) proliferation and collagen formation. To understand the cardioprotective effect of CCDC80tide, a transcriptomic analysis reveals a dramatic inhibition of the STAT3 (Signal transducer and activator of transcription 3) signaling pathway in CCDC80tide overexpressing cells. Mechanistically, CCDC80tide selectively interacts with the kinase-active form of JAK2 (Janus kinase 2) and consequently inhibits its kinase activity to phosphorylate and activate STAT3.

Interpretation The results provide new insights into exercise-afforded cardioprotection in pathological cardiac remodeling and highlight the therapeutic potential of CCDC80tide in heart failure treatment.

Funding This work was supported by the National Natural Science Foundation of China [Grant/Award Numbers: 81770428, 81830010, 82130012, 81900438, 82100447); Shanghai Science and Technology Committee [Grant/Award Numbers: 21S11903000, 19JC1415702]; Emerging and Advanced Technology Programs of Hospital Development Center of Shanghai [Grant/Award Number: SHDC12018129]; China Postdoctoral Science Foundation [2021M692108]; and China National Postdoctoral Program for Innovative Talents [BX20200211].

Keywords: Cardiac remodeling; Exercise training; Exerkines; STAT3 signaling pathway

Introduction

Heart failure is a leading cause of morbidity and mortality globally.[1] Hypertension contributes significantly to the incidence of heart failure through pathologic left ventricular hypertrophy and diastolic dysfunction.[2–4] Currently, hypertension is highly prevalent in the heart failure population and is the major driver of heart failure in developed countries.[5] Therefore, suppressing

*Corresponding authors at: Department of Cardiology, Shanghai Chest Hospital, Shanghai Jiao Tong University School of Medicine, 241 West Huaihai Road, Xuhui District, Shanghai 200030, China.
E-mail addresses: heben241@126.com (B. He), rjshenlinghong@126.com (L. Shen).
[1] These authors contributed equally to this work.

Research in context

Evidence before this study

Hypertensive cardiac remodeling is the leading cause of heart failure, while effective treatment strategies remain absent. Exercise training confers cardioprotection from pathological cardiac remodeling and heart failure. However, the underlying mechanism is still elusive.

Added value of this study

By performing an integrative analysis of multi-omics data of the skeletal muscle in response to exercise and later validation in humans, we found an exerkine termed CCDC80tide. CCDC80tide protects against angiotensin II (Ang II)-induced cardiac hypertrophy and fibrosis in mice and inhibits a cascade of adverse biological events driven by Ang II. Notably, CCDC80tide selectively interacts with the kinase-active form of JAK2 and consequently sequesters its kinase activity to phosphorylate and activate STAT3.

Implications of all the available evidence

Our study provides new insights into exercise-afforded cardioprotection in pathological cardiac remodeling and offers a potential therapeutic target for heart failure.

hypertensive cardiac remodeling is important in impeding heart failure progression.

The beneficial effects of regular physical activity on the cardiovascular system are well recognized.[6] Physiologically, exercise training improves glucose and lipid homeostasis, which are classic cardiovascular risks. Exercise training also increases parasympathetic tone to reduce resting heart rate, augments flow-mediated vasodilation to improve vascular endothelial function, and triggers vasculogenesis through endothelial progenitor cells. Exercise may mimic the effects of ischemic preconditioning by increasing the accumulation of several metabolites (such as adenosine, bradykinin, opioids, and nitric oxide (NO)) and the antioxidant capacity to improve myocardial tolerance to ischemia and reperfusion injury.[7] In addition, aerobic exercise protects against chemotherapy-induced cardiotoxicity by regulating proapoptotic and autophagy signaling and improving cardiovascular and endothelial function.[8,9]

The positive effects of physical exercise in suppressing cardiac hypertrophy and improving cardiac function have been documented in patients with heart failure.[10,11] Exercise could directly trigger intrinsic myocardial changes, including increased cytosolic antioxidant capacity, mitochondrial biogenesis, and cardioprotective cardiac growth, by activating signaling pathways, such as insulin-like growth factor 1/ Phosphatidylinositol 3-kinase/protein kinase B (IGF1/PI3K/Akt) pathway,[12,13] and modulating gene expression via microRNAs (miR-17-3p, miR-222, etc.),[14–17] which promote physiological cardiac remodeling and resist pathological remodeling.[18–20]

Exercise also orchestrates multisystemic effects, such as cardiovascular adaptions, by provoking the muscle and other tissues to exert endocrine effects and release various signaling molecules named "exerkines" into the circulation.[21–23] Several exerkines including proteins (e.g., HSP70),[24] non-coding RNAs (e.g., miR-342-5p).[25,26] have been found to exert cardioprotective functions in distinct cardiac pathological contexts, such as myocardial ischemia/reperfusion (I/R) and diabetic cardiovascular complications. The majority of exerkines are considered to originate from the skeletal muscle, given that this is the organ undergoing contraction and major disruption to metabolic homeostasis.[27] However, the role and mechanism of exerkines in cardioprotection, particularly in hypertensive cardiac remodeling, are still ambiguous.

Signal transducer and activator of transcription 3 (STAT3) plays a complicated role in cardiovascular function. Canonical phosphorylation at Tyr705 results in STAT3 dimerization and nuclear translocation, which impairs mitochondrial bioenergetics, promotes profibrotic gene expression, and drives cardiac hypertrophy.[28] STAT3 phosphorylation may also interact with SMAD3, which synergistically promotes fibrosis in the heart.[29] Selective inhibition of STAT3 phosphorylation attenuates cardiac fibrosis in a mouse MI model.[30] Conversely, cardiomyocyte-specific knockout of STAT3 results in aggravated cardiac fibrosis in aged mice.[31] STAT3 also protects the heart against I/R injury by preserving mitochondrial function and exerting non-genomic pro-survival functions.[32] Several post-translational modifications of STAT3, including phosphorylation (Y705 and S727),[33] acetylation,[34] and oxidation[35] impact STAT3 localization and favor the STAT3-mediated cardioprotective effects. At present, the spatiotemporal STAT3 dynamics, function, and regulation of STAT3 in diverse cardiac pathophysiological conditions are not fully understood and more research is needed to clarify these issues.

Here, we performed an integrative analysis of multi-omics databases of skeletal muscle in response to exercise, including transcriptome,[36] secreted proteome,[37] and plasma peptidome,[38] to seek potential exerkines. Our results identified a exerkine termed CCDC80tide (a peptide derived from CCDC80, coiled-coil domain-containing protein 80), which can be released into the circulation via extracellular vesicles (EVs) in response to exercise. Overexpression of CCDC80tide protected against Angiotensin Ⅱ (Ang II)-induced cardiomyocyte hypertrophy in vivo and in vitro. This protective effect is mediated by the selective interaction between CCDC80tide and kinase-active form of JAK2 (Janus kinase 2), which in turn blocks JAK2-mediated

activation of STAT3 (Signal transducer and activator of transcription 3) signaling pathway. Our findings present a mechanism underlying exercise-afforded cardioprotection in hypertension and highlight the therapeutic potential of CCDC80tide in hypertensive cardiac remodeling.

Methods

Bioinformatics analysis

For potential exerkine screen, the significantly up-regulated gene lists (Fold change>1.5, P value < 0.05) in response to exercise from transcriptome, secreted proteome, and plasma peptidome are collected for GO analysis, DisGeNET enrichment analysis, and overlapped genes analysis using online tool Metascape (www.metascape.org) based on multiple independent databases studying functional enrichment.

Cell culture and treatment

For primary cardiomyocyte isolation, the hearts of 2-day-old neonatal rats (rats were euthanised by CO2 asphyxiation) were harvested, washed with phosphate buffer saline (SH30256.01, PBS, Hyclone, USA) and minced, and digested with digestion solution containing 0.6% pancreatin and 0.4% collagenase type II (C6885, Sigma-Aldrich, USA) by slow rotation for 30 min at 37°C. Then, supernatants were collected. The abovementioned digestion step was repeated once more to maximize cell isolation. To remove cardiac fibroblasts, the resulting samples were cultured in dish and incubated at 37°C for 2 h; then, the supernatant was collected and centrifuged at 1000 rpm for 5 min. The supernatant was removed, and the pellet was resuspended in Dulbecco's modified Eagle cell culture medium (SH30243.01, DMEM, Hyclone, USA) containing 10% horse serum (26050088, Gibco, USA), 5% fetal bovine serum (10270, FBS, Gibco, USA) and 1% penicillin/streptomycin (15140122, P/S, Gibco, USA).

Cardiac microvascular endothelial cells (CMECs) were isolated from 8-week-old male SD rats. Rats were anaesthetised by isoflurane inhalation (4% in O_2 for induction, 2% in O_2 for maintenance). After rats were anesthetized, hearts were harvested and rinsed with cold PBS. After the epicardial and endocardial surfaces and interventricular septum were removed, hearts were minced and then digested with 0.2% collagenase type I (SCR103, Sigma-Aldrich, USA) and 0.02% trypsin (25300054, Gibco, USA), respectively, for 30 min at 37°C. After digestion was terminated, the suspension was filtered through a 100-μm strainer (BD Biosciences, USA) and then centrifuged at 1000 rpm for 7 min. The cell pellet was resuspended and cultured in endothelial cell medium (1001, ScienCell, USA) supplemented with 5% FBS and 1% endothelial cell growth supplement. After 4 h, the culture medium was exchanged for fresh medium.

Vascular smooth muscle cells (VSMCs) were isolated from 6–8-week C57BL/6J mice. The thoracic aortas of mice were harvested and rinsed. The adventitia of the thoracic aortas was removed, and vessels were cut into small pieces. The tissues were spread evenly over the cell culture dishes and placed upside down in the incubator. The culture medium was added when the dishes were dry. VSMCs migrated out from tissue fragments after several days. The cells were obtained and cultured in DMEM supplemented with 10% FBS and 1% P/S at an atmosphere of 5% CO_2 and 95% air at 37°C.

H9c2, C2C12 and 293T cell lines were cultured in DMEM supplemented with 10% FBS and 1% P/S. AC16 cell line was cultured in DMEM/F12 supplemented with 10% FBS and 1% P/S. The cell lines were all cultured at an atmosphere of 5% CO_2 and 95% air at 37°C.

In vivo study

Eight-week-old C57BL/6 male mice (22–25 g) were obtained from Charles River Laboratory Animal Technology (Beijing, China). Mice were kept in SPF rooms with abundant food and water. Mice were anaesthetised by isoflurane inhalation (4% in O_2 for induction, 2% in O_2 for maintenance). Tramadol (20 mg/kg) was administrated intraperitoneally to mice undergoing surgery for postoperative analgesia. Mice were euthanised by CO2 asphyxiation. The random number table method is used for the grouping of mice and the double-blind method is used for evaluation. For each experimental group, there are no exclusions of experimental units or data points in the analysis. The number of animals was determined through power analysis and the principle of 3Rs.

For swim training, the protocol refers to previous reports.[25] Eight-week-old male mice were forced to swim 5 days per week for 3 months. In the first week, mice swam for 30 min per day and then gradually increased to 60 min per day. The water temperature was 33°C-35°C. Control groups mice were raised normally without swimming training (n=7 *per* group, total number: 14). All mice ate food and drank water freely. After complete swimming training, the skeletal muscle of mice were collected for western blot analysis.

For CCDC80tide intervention assay, mice were randomly divided into four groups: vehicle group, CCDC80tide group, angiotensin II + vehicle (Ang II + vehicle) group, and Ang II + CCDC80tide group (n=9 *per* group, total number: 36). CCDC80tide (AAV9-cTNT-m-CCDC80tide-HA-EGFP, 1.5×10^{12} vg/mL) and vehicle (AAV9-cTNT-EGFP, 1.0×10^{12} vg/mL) adenoviruses (AAV) were injected through the tail veins (1×10^{11} vg/mL per mouse). Eighteen days after injection, mice were implanted an osmotic pump (model

2004, ALZET, USA) through the subcutaneous route dorsally to continuously receive Ang II infusion (1.5 mg/kg/day, A9525, Sigma-Aldrich, USA) for 4 weeks. Then, blood pressure was measured through the Blood Pressure Meter (BP-2010, Softron, Japan), and the ultrasonic Vevo 770 high-resolution imaging system (VisualSonics, Canada) was used to assess cardiac function. After sacrifice, the hearts were harvested and subjected for histopathology detection and WB analysis.

Frozen sections of the hearts were obtained, and fluorescence detection was performed to assess the efficiency of AAV infection. Paraffin sections were subjected for hematoxylin and eosin (H&E) staining, Masson's trichrome staining, wheat germ agglutinin (WGA) fluorescent staining, and immunohistochemistry staining (CD31). Cardiomyocyte cross-sectional areas were measured from randomized images of 100 cells by ImageJ software. Cardiac fibrotic area was quantified by blue areas divided by the total areas in each section. Capillary density was quantified from at least three fields per slide and two slides in each animal.

Subjects and exercise protocol

All human studies adhered to the Declaration of Helsinki principles. Informed consent was obtained from all participants. Participants were informed about the procedures and possible risks with the study. Twenty healthy subjects, including 10 males and 10 females, in good health, with no history of cardiovascular diseases, free of medication and substance abuse, and physically normal (exercise 2–3 times a week) were recruited. The characteristics of participants are listed as Table 1. Volunteers fasted overnight (10–12 h) and rested for 30 min. Fasting blood samples were obtained from the forearm vein and collected in purple tube vacutainers (K2EDTA, BD, USA). Participants were encouraged to run at a gradually increasing velocity and run for about 10 min at the maximal exercise capacity. Intravenous blood samples were collected at baseline (before exercise), the last minute of exercise, and 2 h after exercise. Blood samples were centrifuged at 1600 g at 4°C for 10 min. The EDTA plasma was transferred to a new tube and stored at 4 °C for isolation immediately.

Extracellular vesicles (EVs) isolation

The EVs were isolated from C2C12 media as previously described.[39] C2C12 (RRID:CVCL_0188) mouse myoblasts were cultured in DMEM supplemented with 10% FBS and 1% P/S. When the cells reached a density of 100%, the culture medium was exchanged for differentiation medium (DMEM supplemented with 2% horse serum) for 1 week. Then, the culture medium was exchanged for differentiation medium with exosome-depleted FBS (EXO-FBS-50A-1, SBI, USA) for 48 h. The culture supernatants (10 ml *per* dish) were harvested for and centrifuged at 2000 g for 30 min to remove cells and debris. Then, supernatants were used for EVs isolation immediately using a Total Exosome Isolation Kit (4478359, Invitrogen, USA) according to the manufacturer's manual. In brief, the supernatants were transferred to a new tube and add 0.5 volumes of the Total Exosome Isolation reagent. Then, mix the culture media/reagent mixture well by pipetting up and down until there is a homogenous solution. The mixture samples were incubated at 4 °C overnight. After incubation, centrifuge the samples at 10,000 × g for 1 hour at 4°C. Discard the supernatant, and EVs are collected by resuspending the pellet at the bottom of the tube. The EVs-derived proteins were extracted using exosome protein lysate (UR33101, Umibio, China). The obtained protein was subjected for subsequent Western blot (WB) analysis, Nanoparticle Tracking Analysis (NTA, ZetaView PMX110, Particle Metrix), and transmission electron microscope (TEM, G2 Spirit FEI, Tecnai) analysis.

For plasma EVs isolation, EVs was extracted immediately according to the instructions of Total Exosome Isolation (from plasma) Kit (4484450, Invitrogen, USA). Plasma samples were centrifuged at 2000 × g for 20 min at room temperature. Then, transfer the supernatant to a new tube and centrifuged at 10,000 × g for 20 min at room temperature. The supernatant was collected and 0.5 volumes of 1 × PBS and 0.05 volumes of Proteinase K were added. Then, vortex the sample mixture and incubate at 37°C for 10 min. Then, Exosome Precipitation Reagent was added to samples and incubation at 4°C for 30 min. After incubation, centrifuge the sample at 10,000 × g for 5 minutes at room temperature. Discard the supernatant, and EVs are collected by

	Baseline		Post-exercise (3 min)	
Variables	**Males**	**Females**	**Males**	**Females**
Age (years)	25.5 ± 0.7	25.2 ± 0.8		
Body mass index (kg/m^2)	22.1 ± 1.2	19.5 ± 1.1		
Systolic blood pressure (mmHg)	118.7 ± 5.7	112.8 ± 5.9	132 ± 5.9	121.4 ± 7.4
Diastolic blood pressure (mmHg)	74.2 ± 7.2	70.8 ± 5.0	82.5 ± 6.2	75.6 ± 4.9
Heart rate (min^{-1})	79 ± 5.4	82.4 ± 4.5	111.6 ± 6.4	120.2 ± 6.3

***Table 1*: The characteristics of participants.**

resuspending the pellet at the bottom of the tube. The proteins in EVs were extracted using exosome protein lysate (UR33101, Umibio, China). The concentrations of CCDC80tide in EVs were measured by ELISA (Human CCDC80 ELISA Kit, EK1962, Boster Bio, USA) combined with immunoblotting assay.

Western blot analysis

After treatment, cells were washed with cold PBS and lysed with RIPA buffer (P0013B, Beyotime Biotechnology, China) on ice for 30 min and then centrifuged at 12000 rpm at 4°C for 30 min. The supernatant was collected, and the protein concentration was measured by BCA Protein Assay Kit (23225, Thermo Fisher Scientific, USA). A 30-μg aliquot protein was separated on Sodium dodecyl sulfate-polyacrylamide gel electrophoresis (SDS-PAGE) gel and transferred to PVDF membranes (Millipore, USA). The membranes were blocked with 5% skimmed milk and incubated with primary antibody at 4°C overnight. After washing with TBST, the membranes were incubated with horseradish peroxidase-linked secondary antibody at room temperature for 1 h. The membranes were developed with Immobilon Western HRP Substrate (WBKLS0500, Millipore, USA) and Amersham Imager 680 (Cell Signaling Technology, USA)

The antibodies used were as follows: anti-CCDC80 (AF3410, R&D, USA, RRID:AB_2072229), anti-PGC1α (66369-1-Ig, Proteintech, USA, RRID:AB_2828002), anti-GAPDH (5174, Cell Signaling Technology, USA, RRID:AB_10622025), anti-TSG101 (ab125011, Abcam, USA, RRID:AB_10974262), GM130 (11308-1-AP, Proteintech, USA, RRID:AB_2115327), GRP94 (14700-1-AP, Proteintech, USA, RRID:AB_2233347), anti-CD9 (13403, Cell Signaling Technology, USA, RRID:AB_2732848), anti-HA Tag (3724, Cell Signaling Technology, USA, RRID:AB_1549585), anti-HA Tag (HRP conjugate) (2999, Cell Signaling Technology, USA, RRID:AB_1264166), anti-DYKDDDDK (8146, Cell Signaling Technology, USA, RRID:AB_10950495), anti-MYH7 (22280-1-AP, Proteintech, USA, RRID:AB_2736821), anti-collagen type I (14695-1-AP, Proteintech, USA, RRID:AB_2082037), anti-TGF-β1 (21898-1-AP, Proteintech, USA, RRID:AB_2811115), anti-STAT3 (9139, Cell Signaling Technology, USA, RRID:AB_331757), anti-P-STAT3(Y705) (9145, Cell Signaling Technology, USA, RRID:AB_2491009), anti-JAK2 (3230, Cell Signaling Technology, USA, RRID:AB_2128522), anti-P-JAK2(Y1007/1008) (3771, Cell Signaling Technology, USA, RRID:AB_330403), anti-vascular cell adhesion molecule-1 (VCAM-1) (ab134047, Abcam, USA, RRID:AB_2721053), anti-intercellular adhesion molecule-1 (ICAM-1) (10020-1-AP, Proteintech, USA, RRID:AB_2121773), anti-MMP9 (2270, Cell Signaling Technology, USA, RRID:AB_2144612), anti-α-smooth muscle actin (ab7817, Abcam, USA, RRID:AB_262054), and anti-β-tubulin (T0023, Affinity, USA, RRID:AB_2813772).

Real-time fluorescence quantitative polymerase chain reaction (qPCR) and reverse transcription PCR (RT-PCR)

For qPCR analysis, total RNA was extracted using TRIzol (10296028, Invitrogen, USA) and reverse transcribed into cDNA using PrimeScript RT Master Mix (RR036A, Takara, Japan). Amplification for RT-PCR was conducted using TB Green (RR420B, Takara, Japan) and analyzed by the 7300 Plus Real-Time PCR System (Thermo Fisher Scientific, USA). The primers used in the study were shown in Table 2. The holding stage was 95°C for 30 s, followed by 40 cycles of cycling stage (95°C for 5 s, 60°C for 1 min) and melt curve stage (95°C for 15 s, 60°C for 1 min, 95°C for 15 s, 60°C for 15 s).

For RT-PCR analysis, total RNA was extracted from the tissues and reverse transcribed. Then, cDNAs were amplified using PrimeSTAR Max DNA Polymerase (R045A, Takara, Japan) and Biometra Thermal Cycler

Gene	Forward Seuence (5′ to 3′)	Reverse Seuence (5′ to 3′)
Rat-β-MyHC	GAGCCTCCAGAGTTTGCTGAAGGA	TTGGCACGGACTGCGTCATC
Rat-Tgf-β1	AAACGGAAGCGCATCGAA	GGGACTGGCGAGCCTTAGTT
Rat-Col1a1	TGACCTCAAGATGTGCCACT	ACCAGACATGCCTCTTGTCC
Rat-GAPDH	ATGGTGGTGAAGACGCCAGTA	GGCACAGTCAAGGCTGAGAATG
Rat-Vcam-1	ATGCCTGGGAGGATGGTCGC	CAGGAGCCAAACACTTGACC
Rat-Icam-1	TGTCGGTGCTCAGGTATCCATCC	TTCGCAAGAGGAAGAGCAGTTCAC
Mouse-Pgc-1α	TCACACCAAACCCACAGAAA	TCTGGGGTCAGAGGAAGAGA
Mouse-CCDC80	CGTGAGATGGTCCGAGATGA	CCAGCTCACAATACACGTCG
Mouse-Col1a1	ACATGTTCAGCTTTGTGGACC	TAGGCCATTGTGTATGCAGC
Mouse-Fn-1	TTAAGCTCACATGCCAGTGC	TCGTCATAGCACGTTGCTTC
Mouse-Mcp-1	AGGTCCCTGTCATGCTTCTG	TCTGGACCCATTCCTTCTTG
Mouse-Spp-1	ATTTGCTTTTGCCTGTTTGG	TGGCTATAGGATCTGGGTGC
Mouse-β-actin	AGGTGACAGCATTGCTTCTG	GCTGCCTCAACACCTCAAC

***Table 2*: The primers used in this study.**

(Analytik Jena, Germany). The initial step was 98°C for 3 min, 30 cycles of the amplification step (98°C for 10 s, 50°C for 5 s, 72°C for 20 s) and followed by another step (72°C for 10 min). The PCR products were run on 2% agarose gel electrophoresis to compare the expression levels.

Immunoprecipitation (IP)

Total protein was extracted from cells with lysis buffer (50 mM Tris-HCL, pH 7.5, 150 mM NaCl, 0.5% NP-40) and then incubated with corresponding tag beads at 4°C overnight. The supernatant was discarded, and the beads were washed six times with lysis buffer. The beads were eluted with 2 × SDS loading buffer at 95°C; then, the supernatant was collected as immunoprecipitates, which were separated on SDS-PAGE gels.

Cell proliferation assay

Cell proliferation was detected using Cell Counting Kit-8 (CK04, Dojindo, Japan) according to the introductions. Briefly, VSMCs were seeded in 96-well microplates. After incubation at 37°C and 5% CO_2 for 24, 48, and 72 h, the culture medium of each well was replaced with fresh medium containing 10% CCK-8 reagent and incubated at 37°C for 30 min, the microplate was measured with absorbance at 450 nm through multimode microplate reader (Varioskan LUX, Thermo Fisher Scientific, USA).

ROS assay

CellROX Reagent (M36008, Invitrogen, USA) was added to cells at a final concentration of 5 μM. After incubation at 37°C for 30 min, the cells were washed three times with PBS and fixed with 4% paraformaldehyde for 10 min and DAPI (C1002, Beyotime, China) was used to mark the nuclei. Cells were observed and photographed through a fluorescence microscope (Leica, Germany).

Gene overexpression and knockdown

The CCDC80, △DUDES-CCDC80, JAK2, JAK2 (K882E), and PGC-1α were constructed into the pHAGE vector with Flag, HA, or EGFP tag. Lentivirus production using the pHAGE system was used. Briefly, pHAGE expression vectors were co-transfected with packaging vectors into 293T cells (RRID:CVCL_0063), and the resulting supernatants were collected and filtered using a 0.22-um filter (Life sciences, USA) after 48 h. For gene overexpression, lentivirus infection was performed in targeted cells by supplementation of 8 μg/mL polybrene.

For knockdown studies, primary cardiomyocytes were transfected with control or STAT3 siRNAs using Lipo3000 reagent (L3000008, Invitrogen, USA) according to the instruction. The sequence for the STAT3 siRNAs are as follows: siRNA1, GACUUUGAUUUCAACUAUAAAAC; siRNA2, UUGAAUUAUCAGCUUAAAAUUAA; and non-targeting siRNA, UUCUCCGAACGUGUCACGUTT (Table 2). The siRNAs were purchased from TsingKe Biological Technology (Shanghai, China).

Supernatant protein extraction

The cell culture medium was changed to DMEM with 1% FBS for 24 h. The supernatant was collected and centrifuged at 800 g for 2 min and then transferred to a new tube. The trichloroacetic acid (T0699, TCA, Sigma-Aldrich, USA) was added to the supernatant to make a final concentration of 15%. After mixing well, the mixture was placed on ice for 5 min and then centrifuged at 16000 g for 5 min at room temperature. After the supernatant was discarded, the pellet was resuspended with 1% SDS for SDS-PAGE analysis.

Rhodamine-phalloidin staining

After the indicated treatment, cells were fixed with 4% paraformaldehyde and washed four times with washing buffer (PBS containing 0.1% Triton X-100). Cells were incubated in staining solution (5% bovine serum albumin [ST023, BSA, Beyotime, China], 0.1% Triton X-100 and 1% Actin-Tracker Red-Rhodamine [C2207S, Beyotime, China]) in the dark at room temperature for 60 min.

Immunocytofluorescence

Cells were seeded on slides and, after the indicated treatment, were washed with PBS twice and fixed with 4% paraformaldehyde at room temperature for 15 min. Then, 0.2% Triton-100 was used to permeabilize cells for 10 min, followed by blocking with 5% BSA for 30 min at room temperature. Cells were incubated with primary antibodies diluted in 2% BSA at 4°C overnight. Next day, cells were washed with PBS four times and incubated with corresponding secondary antibodies diluted in 2% BSA in the dark for 30 min at room temperature. Then, cells were washed with PBS and stained with DAPI. The slides were sealed with anti-fluorescence quenching sealing tablets, and observations were performed under microscope.

RNA-sequencing (RNA-seq)

For RNA-seq analysis, total RNA was extracted using TRIzol and further purified using RNAClean XP Kit (Beckman Coulter, USA) and RNase-Free DNase Set (QIAGEN, Germany). RNA was qualified through NanoDrop ND-2000 spectrophotometry and Agilent Bioanalyzer 2100 (Agilent Technologies, USA). After the total RNA was reversed and amplified, transcriptome sequencing libraries were constructed by VAHTS

mRNA-seq v2 Library Prep Kit for Illumina (Vazyme, China). Transcriptome sequencing was conducted using a high-throughput sequencer (Illumina Hiseq 2500). Further analysis was performed using online tool Metascape (http://metascape.org/).

Statistical analysis

All statistical analyses were performed using SPSS software (SPSS Inc.) and the GraphPad Prism 8 (GraphPad Software). The experiments were repeated independently at least three times. The data were shown as mean ± SD. Student's t-test or one-way ANOVA with Tukey's post hoc test was used to assess statistical differences between each group. A p-value of <0.05 indicated significance.

Ethics

All human studies were approved by Shanghai Chest Hospital Ethics Committee (approval number: IS2166). The study adhered to the Declaration of Helsinki principles. All animal experiments were conformed to the National Institutes of Health Research Guidelines on the Care and Use of Laboratory Animals and approved by the respective authorities of Shanghai Jiaotong University (approval number: KS(Y)21282).

Role of Funders

The funding sources played no role in study design, data collection, data analyses, interpretation, or writing.

Results

CCDC80 is a potential exerkine involved in cardiovascular pathophysiology

Gene Ontology (GO) analyses based on previously reported transcriptome,[36] secreted proteome,[37] and plasma peptidome[38] data derived from the exercise-stimulated skeletal muscle highlighted the enrichments of several biological pathways involved in the extracellular matrix (ECM) functions and Insulin-like growth factor 2 (IGF2) signaling pathway in the cohort of upregulated genes (Figure 1a–c). According to the analysis on DisGeNET, upregulated genes show a significant association with cardiovascular diseases, such as thrombophilia, cardiomyopathy, and acute myocardial infarction (Figure 1d).

Among the upregulated genes, a total of five synchronized genes were identified: including collagen alpha-1(III) chain (COL3A1), IGF2, vascular endothelial growth factor C, CCDC80, and collagen alpha-2(V) chain (COL5A2) (Figure 1e). Of note, CCDC80 has a particularly high expression in the vessel, heart, and skeletal muscle (Figure 1f). Moreover, clinical evidence revealed that CCDC80 expression was significantly increased in patients with pulmonary arterial hypertension and heart failure.[40–42] This evidence indicates a close association between CCDC80 and cardiovascular system.

Then, we determined whether CCDC80 upregulation is a response to exercise. Peroxisome proliferator-activated receptor gamma coactivator 1-alpha (PGC-1α) is induced by physical activity in the skeletal muscle, and its level increase is responsible for many of the best known benefits of endurance training, such as fiber-type switching, mitochondrial biogenesis, and resistance to muscle atrophy.[43–45] Thus, we adopted a previously described method that overexpresses PGC-1α to mimic the biological events induced by exercise.[37] Significantly, C2C12 cells overexpressing PGC-1α showed a CCDC80 level of about eightfold higher than in control cells (Figure 1g–h). To further assess the association between muscle CCDC80 expression and exercise training *in vivo*, mice were subjected to 3-month swim exercise and then the level of CCDC80 in skeletal muscle was determined. Consistently, the content of CCDC80 increases simultaneously with that of PGC-1α in skeletal muscle in exercised mice, suggesting muscle CCDC80 responds tightly to exercise stimuli. Thus, these findings suggested that CCDC80 may be a exerkine involved in cardiovascular pathophysiology.

CCDC80 generates a peptide encapsulated in EVs in response to PGC-1α overexpression

CCDC80 is located at the ECM and could be secreted into the medium.[46–48] To determine the distribution of CCDC80 after exercise, PGC-1α was overexpressed, and the intracellular and secreted CCDC80 levels were determined respectively. For the intracellular part, PGC-1α-overexpressing C2C12 cells showed a dramatic increase in the full-length CCDC80 protein levels, while both of the full-length CCDC80 and 45-kDa truncated CCDC80 were detected in the culture medium (Figure 2a). The supernatant full-length and truncated CCDC80 were totally erased by the administration of brefeldin A (HY-16592, BFA, MCE), an inhibitor of protein secretion[49] (Figure 2a). We observed that the band for CCDC80 from the medium is shifted up compared with the band for CCDC80 from cell lysates. This may be due to glycosylation during CCDC80 secretion,[48] which is required for protein folding and secretion. To monitor the behavior mode of secreted CCDC80, C-terminal GFP tagged CCDC80 (to circumvent the signal peptide located at the N-terminus) was transfected into C2C12 cells, and the supernatant was collected and added into the culture of H9c2 cells (RRID: CVCL_0286). Interestingly, fluorescent signals were widely detected within H9c2cells (Figure 2b). To monitor instinct distribution of CCDC80, the C-terminal GFP tagged CCDC80 was overexpressed into H9c2 cells, and the fluorescence was distributed in the

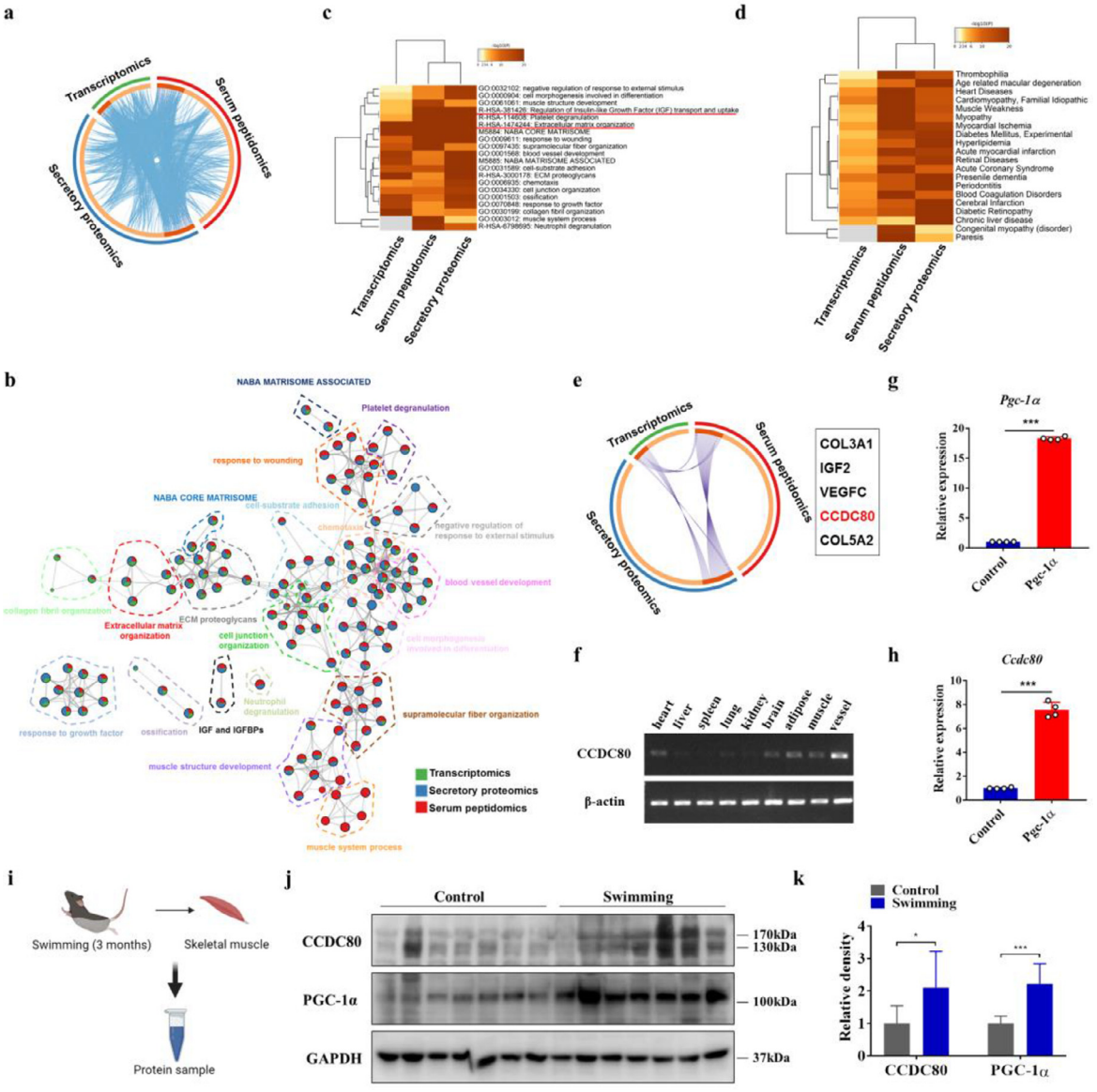

Figure 1. CCDC80 is a potential exerkine involved in cardiovascular pathophysiology.

a. Circos plot visualizes the overlap between upregulated gene lists from three databases, and the blue curves link genes that belong to the same enriched GO term.

b. Pie charts represent the network of enriched terms in upregulated genes. Each circle node represents an enriched term and is clustered by its identity, where the size of a slice represents the percentage of genes under the term that originated from the corresponding database.

c. Heatmap of enriched terms across the three upregulated gene lists, colored by *p*-values.

d. Heatmap of enrichment analysis in DisGeNET, colored by p-values.

e. Circos plot displays the overlap between upregulated gene lists, and the purple curves link identical genes. The five genes within the black box represent the genes with significant upregulation throughout the three databases.

f. RT-PCR analysis of the expression levels of CCDC80 in various tissues of mice.

g, h. After overexpression of PGC-1α in C2C12 cells, the expressions of *Pgc-1α* (g) and *Ccdc80* (h) was determined by qPCR.

i, j and k. Eight-week-old male mice were forced to swim 5 days per week for 3 months. Control groups mice were raised normally without swimming training. After complete swimming training, the skeletal muscles of mice were collected for western blot analysis of CCDC80 and PGC-1α (*n*=7).

Data are presented as the average of four biological replicates (n = 4) $\pm$ SD.

Statistical significance was determined using Student's t-test, ***$p < 0.001$.

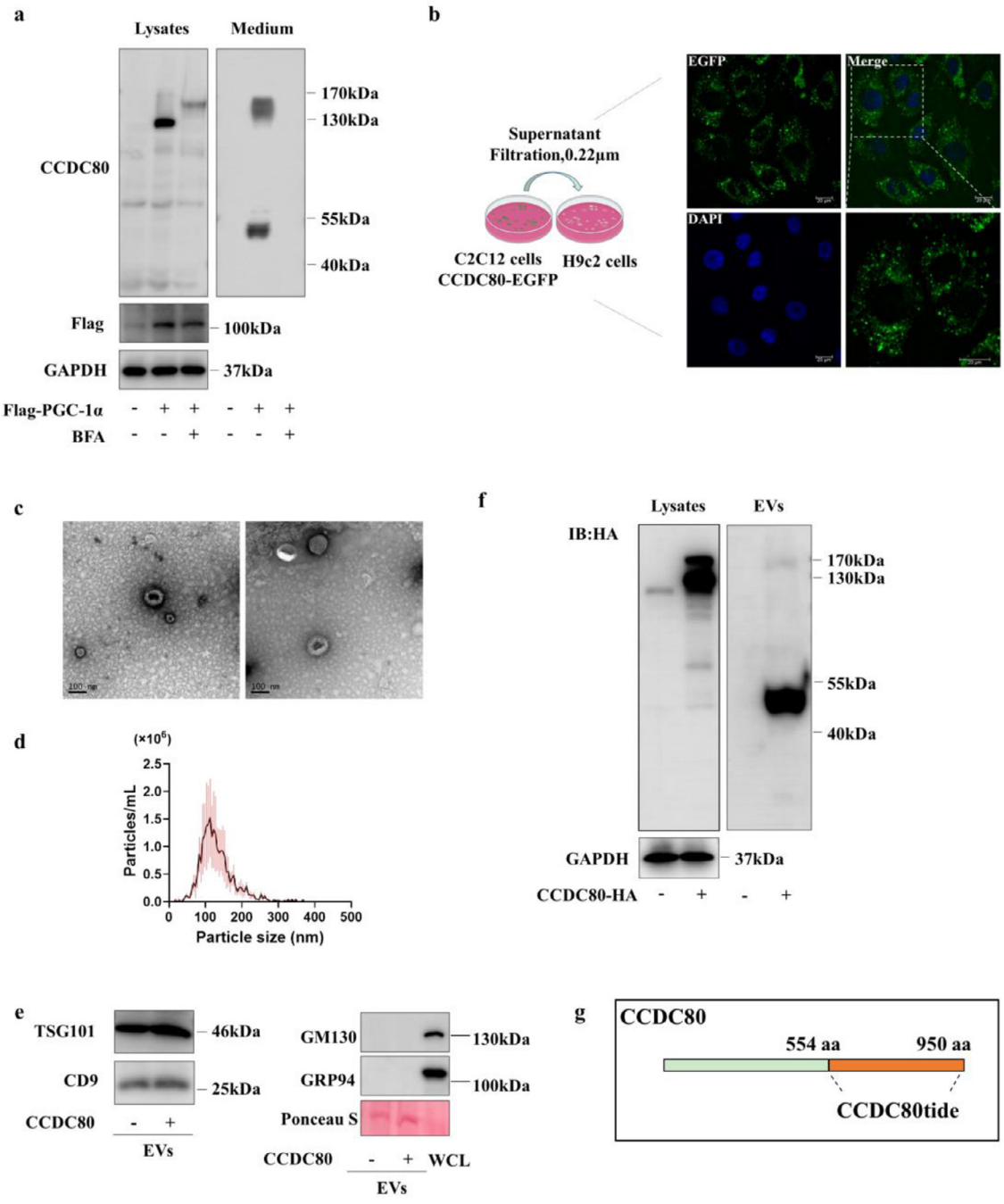

Figure 2. CCDC80 generates a peptide encapsulated in EVs in response to PGC-1α overexpression.

a. The cell lysates and culture supernatants collected from vehicle- or Flag-PGC-1α-overexpressing C2C12 cells (treated or not with BFA, 1 μg/mL, 16 h) were prepared and analyzed for CCDC80 protein levels by WB. *N*=3

b. The supernatants of CCDC80-EGFP-overexpressing C2C12 cells were harvested and filtered through a sterile 0.22-μm filter and then added to H9c2 cells. After 12-h incubation, the cell fluorescence was detected. The fluorescent spots indicated by white arrows were supposedly EVs. *N*=3

c, d, e. The supernatants of CCDC80-overexpressing C2C12 cells were collected, and EVs were extracted for TEM (c), NTA (d), and EVs markers (e) determinations. *N*=3. WCL: whole cell lysates.

f. The cell lysates and EVs isolated from the supernatants of vehicle- or CCDC80-HA-overexpressing C2C12 cells were prepared and analyzed for CCDC80 protein levels by WB.

g. The schematic diagram of CCDC80tide in CCDC80.

cytoplasm and nucleus (Supplemental figure 1). The perinuclear region was also stained in a pattern suggestive of the endoplasmic reticulum and/or Golgi apparatus, the place for CCDC80 processing and secretion.[48,50]

Since naked proteins could not penetrate into cells directly, we speculated that secreted CCDC80 may be encapsulated into extracellular vesicles, especially possible in EVs. This is because the supernatants were filtrated through a 0.22-μm membrane filter before utilization. To confirm this possibility, we collected the supernatants of CCDC80-overexpressed C2C12 cells and extracted EVs for identification. The morphology, diameter, and number of EVs were examined using a Transmission electron microscope (TEM) and Nanoparticle Tracking Analysis (NTA), respectively. As shown in Figure 2c–d, EVs displayed a spherical shape, approximately 111.7 nm (94.6%) in diameter. EVs were also verified by detecting EVs markers CD9 and TSG101, and negative markers GRP94 and GM130 (Figure 2e). Next, the EVs were subjected to WB analysis using CCDC80 antibody. Surprisingly, there is an apparent enrichment of the 45 kDa truncated CCDC80 in EVs (Figure 2f). To dissect this fragment, the amino acid sequences of this fragment were identified by mass spectrometric analysis and revealed that it was located in the range of the C-terminal 554-950 aa of CCDC80 (Figure 2g, supplemental figure 2a). The sequence alignments revealed high identity (96.24%) in human, mouse, and rat, indicating the crucial evolutionarily conserved functions of this fragment (Supplemental figure 2b). Collectively, exercise-related PGC-1α activation leads to the secretion of the C-terminal fragment of CCDC80 through EVs. To facilitate a subsequent study, this fragment was named as CCDC80tide (CCDC80-derived peptide).

Acute exercise stimulates the rapid release of CCDC80tide into the circulation in humans

Acute physical activity triggers the rapid release of EVs that leads to several changes in metabolic and cardiovascular pathways.[51] We speculated whether CCDC80tide concentration could be provoked in response to acute exercise in humans. Ten healthy male and ten healthy female volunteers were recruited (Table 1), and the participants were abstained from strenuous exercise for 2 days and fasted overnight before the experiment. The venous blood samples were collected before (rest), immediately after (exercise), and 2 h after (recovery) an acute treadmill exercise (Figure 3a). Plasma EVs were isolated and identified (Figure 3b-3d), and the contained proteins were extracted for WB analysis using an anti-CCDC80 antibody. Consistently, there is a clear band at approximately 45 kDa, which was in accordance with the molecular size of CCDC80tide (Figure 3d). ELISA assay showed that the concentration of EVs-derived CCDC80tide in exercise samples (men: 13.11± 1.97 pg/mL, women: 14.71±1.58 pg/ml) was elevated compared with that of the remaining samples, whereas, in recovery samples (men: 10.94±2.48pg/ml, women: 13.02±1.92 pg/ml), it declined to the level a slightly higher than baseline (men: 9.37±1.98 pg/ml, women: 11.04±1.49 pg/ml) (Figure 3e-3f). Thus, these results suggest that circulating CCDC80tide could be rapidly provoked in response to acute exercise in humans.

CCDC80tide protects against angiotensin II (Ang II)-induced cardiac remodeling

To assess the role of CCDC80tide in pathological cardiac remodeling, an AAV of serotype 9 expressing CCDC80tide under the control of the cardiac-specific cardiac troponin T (cTNT) promoter (AAV9-cTNT CCDC80tide-HA) was intravenously injected into mice. The equal amounts of AAV vehicle was also injected as a control. Eighteen days after injection, mice were chronically treated with Ang II pump for 4 weeks to induce hypertensive cardiac remodeling. After the experiment, we first checked the expression efficiency of CCDC80tide. As expected, the highest expression of CCDC80tide was detected in the heart and the overexpression of CCDC80tide was detected throughout the Ang II treatment. (Figure 4a, Supplemental Figure 3). Visibly, CCDC80tide mitigated Ang II-induced cardiac hypertrophy and increase of heart weight (HW) by measuring HW-to-body weight ratios (HW/BW) (Figure 4b–c). Meanwhile, the systolic blood pressure was lower in CCDC80tide-treated mice compared with that in vehicle-treated mice 1 month after Ang II infusion (Figure 4d). Echocardiography examination revealed that CCDC80tide protected against Ang II-induced loss of cardiac function by inhibiting an increase in left ventricular (LV) mass, left ventricular posterior wall (LVPW), and ventricular wall thickness (Figure 4e–h). Histologically, there was not only prominent concentric change in LV mass but also exacerbation of perivascular and interstitial fibrosis in Ang II-treated mice compared to those in control mice as measured with H&E and Masson staining (Figure 4i–j). In contrast, these unfortunate changes in the hearts of Ang II-treated mice were reversed by CCDC80tide intervention (Figure 4i–j). Moreover, membrane dye WGA staining and quantitative analysis of cardiac myocyte dimensions in sections revealed a significant inhibition of Ang II-induced cardiac myocyte hypertrophy upon CCDC80tide administration, concomitant with the improvement of capillary rarefaction as examined by an anti-CD31 immunohistochemistry (Figure 4k–l). Consistently, Ang II-increased contents of hypertrophic (MYH7) and profibrotic (COL-1, TGF-β1) markers were reversed by CCDC80tide administration (Figure 4m). Taken together, these results demonstrate that

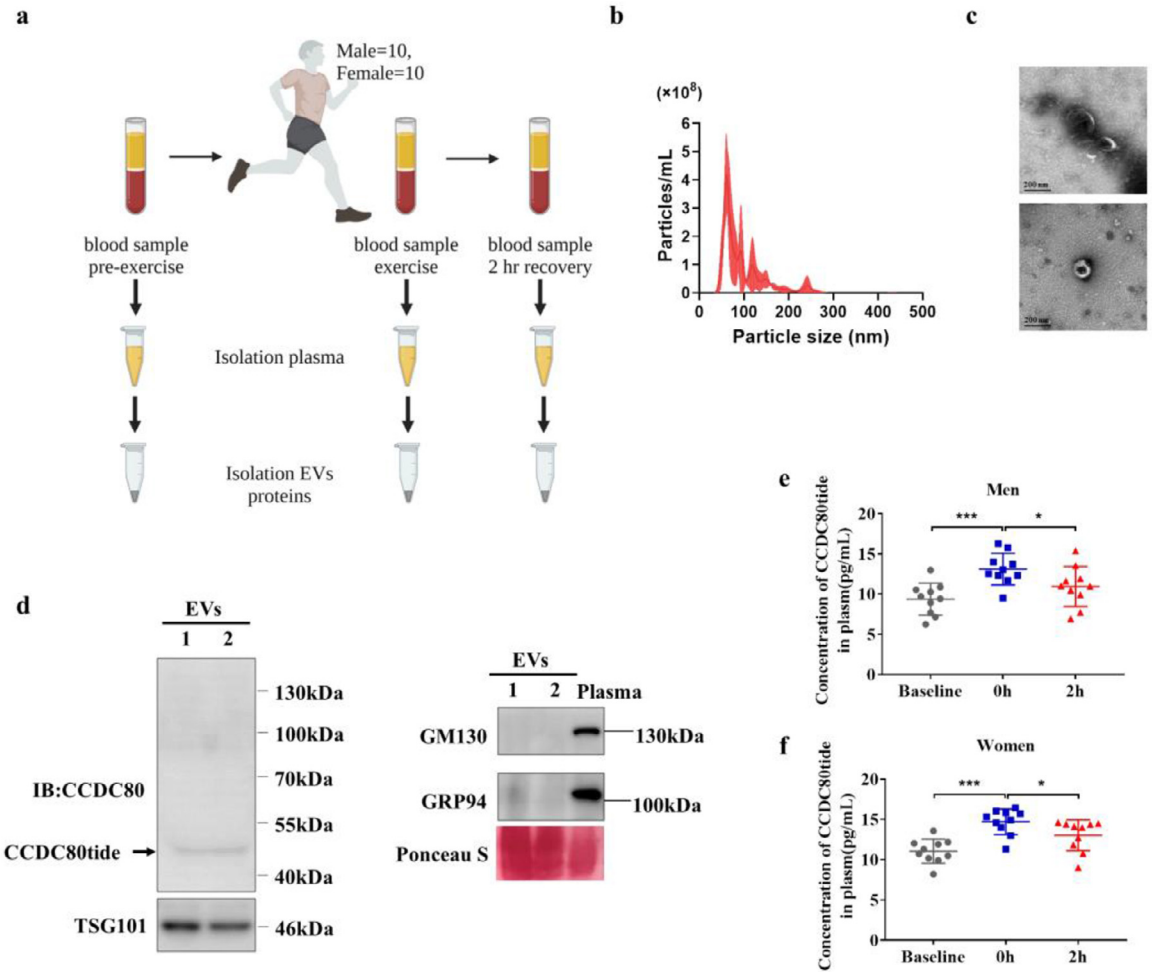

Figure 3. Acute exercise stimulates a rapid release of CCDC80tide into the circulation.

a. Schematic illustration of the experimental design for acute exercise. Twenty subjects (n = 20, males (*n*=10) and female (*n*=10)) were included, and the plasma were obtained before, immediately after, and 2 h after exercise; then, EVs were purified.

b, c. Plasma EVs were extracted for NTA (b) and TEM (c) determinations.

d. The EVs proteins were extracted and analyzed for CCDC80tide and EVs markers by WB.

e, f. The EVs-derived CCDC80tide level was measured by ELISA and represented separately by gender.

Data are presented as mean ± SD, n = 20. Statistical significance was determined using one-way ANOVA with Tukey's post hoc test, $*p < 0.05$.

CCDC80tide alleviates Ang II-induced hypertension, cardiac hypertrophy, and fibrosis.

CCDC80tide opposes Ang II-induced cardiac hypertrophy-related biological events

The pathophysiology of cardiac remodeling is complex and involves numerous biological processes. To explore the biological basis of CCDC80tide-afforded cardioprotection, CCDC80tide was overexpressed in cardiomyocytes and treated with Ang II. The results showed that CCDC80tide dose-dependently reduced the transcriptions of *Myh7*, *Col1a1*, and *Tgf-β* induced by Ang II, and the same trend was observed for the protein contents (Figure 5a–d). Furthermore, rhodamine-phalloidin staining was performed to visualize cardiomyocyte morphology and found that CCDC80tide decreases the enlarged cell size elicited by Ang II (Figure 5e). To check the role of CCDC80tide in human originated cardiomyocytes, AC16 (RRID:4U18) human cardiomyocyte cell line was overexpressed with CCDC80tide and then treated with Ang II. Consistently, as the CCDC80tide content increases, the elevated p-STAT3 and MYH7 induced by Ang II are decreased gradually (Figure 5f). These results suggest that CCDC80tide ameliorates

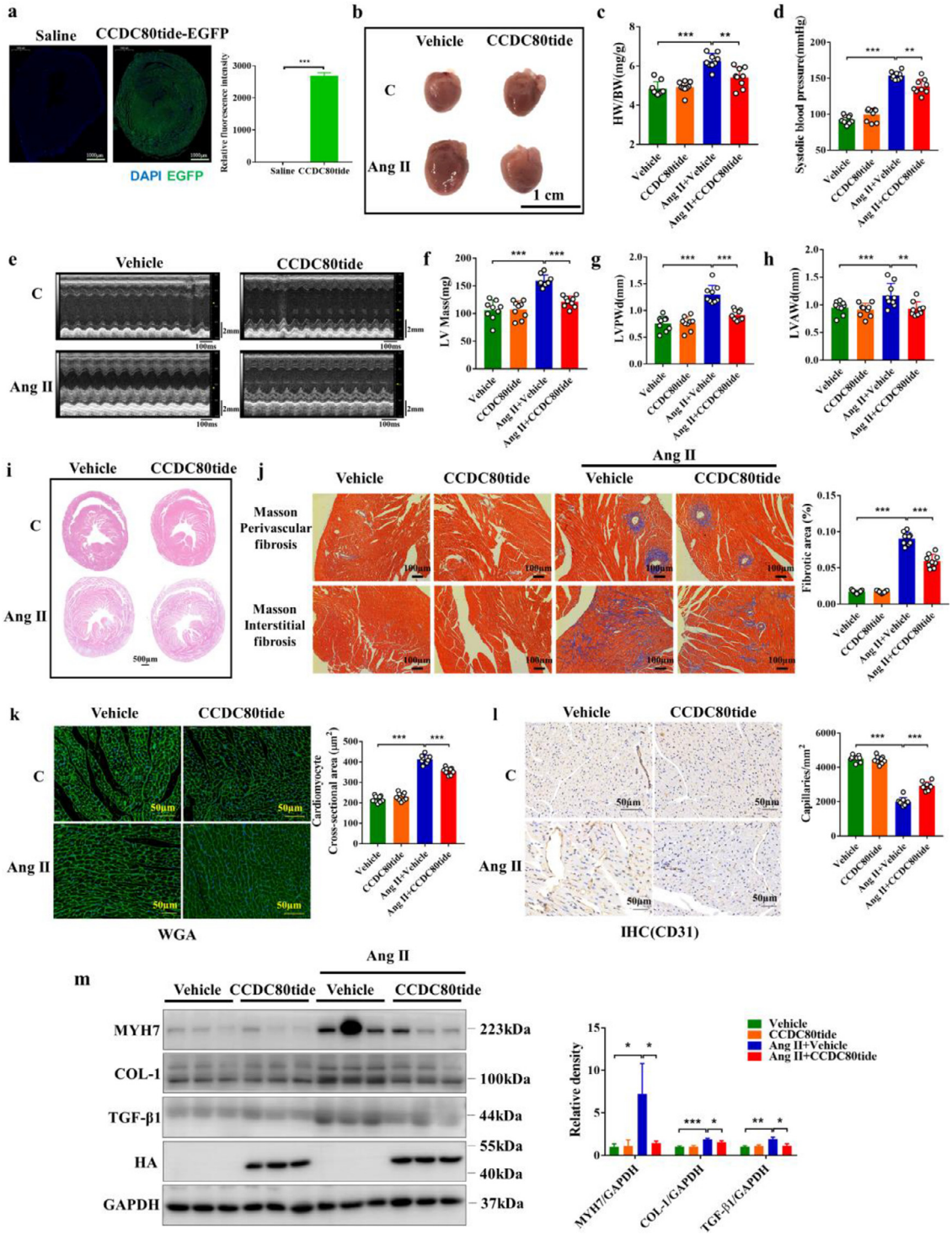

Figure 4. CCDC80tide protects against angiotensin II (Ang II)-induced cardiac remodeling.

AAV9-cTNT CCDC80tide-HA-EGFP was intravenously injected into mice, and the equal amount of AAV9-HA-EGFP vehicle was injected as a control, n = 9 mice per group. Eighteen days after the injection, mice were chronically infused with Ang II (1.5 mg/kg/day) for 4 weeks. Mice were subjected to the following detections upon the termination of the experiment.

a. Left panel, frozen heart tissue sections from AAV9-treated mice were prepared for the detection of EGFP fluorescence. Right panel, the relative quantification of fluorescence intensity. Statistical significance: *** $p < 0.001$ Student t-test.

b. Mice were sacrificed and hearts were dissected, weighed, and photographed.

Ang II-induced hypertrophy in cultured cardiomyocytes.

Vascular endothelial cells (VECs) are the most abundant cell type in the heart in terms of absolute numbers.[52] The disruption of VEC function is involved in the pathogenesis of myocardial hypertrophy.[53] Therefore, we surveyed the role of CCDC80tide in VEC function. The primary CMECs were isolated from rats and identified by staining of von Willebrand factor (Supplemental Figure 4). Endothelial cell adhesion molecules (ECAMs) play crucial roles in the development of chronic inflammation by supporting leukocyte pro-inflammatory behaviors, such as leukocyte rolling, adherence, and emigration in vessels.[54] Our results showed that the expression of CCDC80tide significantly diminished the Ang II-induced expressions of ECAMs, including Vascular cell adhesion molecule-1 (VCAM-1) and Intercellular adhesion molecule-1 (ICAM-1) (Supplemental Figure 5, a–c). Furthermore, CCDC80tide also contributed to redox homeostasis by decreasing the excess accumulation of mitochondrial reactive oxygen species (mtROS) in Ang II exposure (Supplemental Figure 5, d).

Ang II promotes VSMC proliferation and migration and deposition of collagen, which results in vascular injury and remodeling. This plays critical roles in the development of hypertension and cardiac remodeling.[55–57] Proliferation analysis showed a dramatic reduction in Ang II-induced primary VSMC proliferation in CCDC80tide expressing VSMCs (Supplemental Figure 6, a). Moreover, CCDC80tide attenuated the induction of *Col1a1* and *Fn-1* genes in Ang II-treated cells, indicating a decrease in collagen formation (Supplemental Figure 6, b–c). The CCDC80tide treatment also inhibited the increase in *Mcp-1*and *Spp-1* levels, which were important promoters of inflammation and fibrosis (Supplemental Figure 6, d–e). Moreover, the MMP9 level after Ang II exposure decreased along with increase in CCDC80tide level (Supplemental Figure 6, f). Taken together, these data suggest that CCDC80tide protects against a cascade of pathophysiologic processes of hypertensive cardiovascular remodeling *in vitro*.

CCDC80tide ameliorated Ang II-induced hypertrophy through the regulation of STAT3 signaling

To dissect the biological mechanism underlying the cardioprotection effect of CCDC80tide, CCDC80tide-initiated transcriptional programs were surveyed. We performed RNA sequencing using primary cardiomyocytes transiently overexpressed with CCDC80tide to analyze the gene-expression profiles. To minimize the artificial influence and compensative effects, overexpression of CCDC80tide was kept at a low level (four-fold vs. control), and overexpression time was limited to 12 h. Compared to vehicle-overexpressed cells, CCDC80tide-overexpressed cells showed upregulation of 1016 genes and downregulation of 1019 genes ($p < 0.01$) (Figure 6a). Of note, the expressions of S100A4 and collagen genes (Col1a1, Col6a1), all of which play important roles in cardiac fibrosis,[58,59] were significantly downregulated in CCDC80tide-overexpressing cells (Figure 6a). The functional enrichment analysis of differentially expressed genes (DEGs) showed an obvious alteration in cellular metabolism processes, particularly in the lipid metabolism (Supplemental Figure 7). The gene network analysis of DEGs highlighted a considerable downregulation of STAT3 signaling (Figure 6b). Gene-set enrichment analysis (GSEA) also revealed a negative correlation between CCDC80tide overexpression and STAT3 signaling pathway (NES, −1.115, $p = 0.09$) (Figure 6c). To further characterize the dynamic changes of gene expressions at the global level, the DEGs were grouped into six clusters (Supplemental Figure 8, a). Clusters 5 and 6 exhibited a substantial decrease in gene expressions upon CCDC80tide expression. Among these genes, we found a series of genes that are governed by STAT3-mediated transcription, including MMP2 and CCL2, which contribute to cardiac fibrosis (Supplemental Figure 8, b).

Mounting evidence suggests that STAT3 directs remodeling processes in cardiac physiology and pathophysiology through a broad range of cellular and molecular mechanisms, and abnormal activation of STAT3 is involved into cardiac hypertrophy.[60–62]

c. Heart weight (HW), body weight (BW), and heart and body weight ratio (HW/BW). Each dot represents a single animal, the same as below.

d. Before sacrifice, systolic blood pressure was determined by tail-cuff plethysmography.

e, f, g, h. Echocardiography (e) was performed to calculate left ventricular (LV) mass (f), LV posterior wall diastolic (LVPWd) (g), and LV wall thickness (LVAW) (h).

i. HE-stained heart transverse sections of mice treated as indicated.

j. Left panel, heart tissue sections were stained with Masson staining to permit detection of perivascular fibrosis (left upper panel) and interstitial fibrosis (IF, left lower panel). Right panel, fibrotic area (%) was quantified as the ratio of the fibrosis area surrounding the vessel plus interstitial fibrosis to the total tissue area.

k. Left panel, wheat germ agglutinin (WGA)-stained heart sections. Right panel, quantification of cardiomyocyte cross-sectional area.

l. Left panel, immunohistochemical staining for CD31 was performed in sections of mice hearts. Right panel, quantification of capillaries stained with CD31.

m. Left panel, heart lysates were collected and analyzed by WB with the indicated antibodies. Right panel, densitometric quantification of WB.

Data are presented as mean ± SD. Statistical significance (c, d, f, g, h, j, k, i, m) was determined using one-way ANOVA with Tukey's post hoc test. *$p < 0.05$, **$p < 0.01$, ***$p < 0.001$.

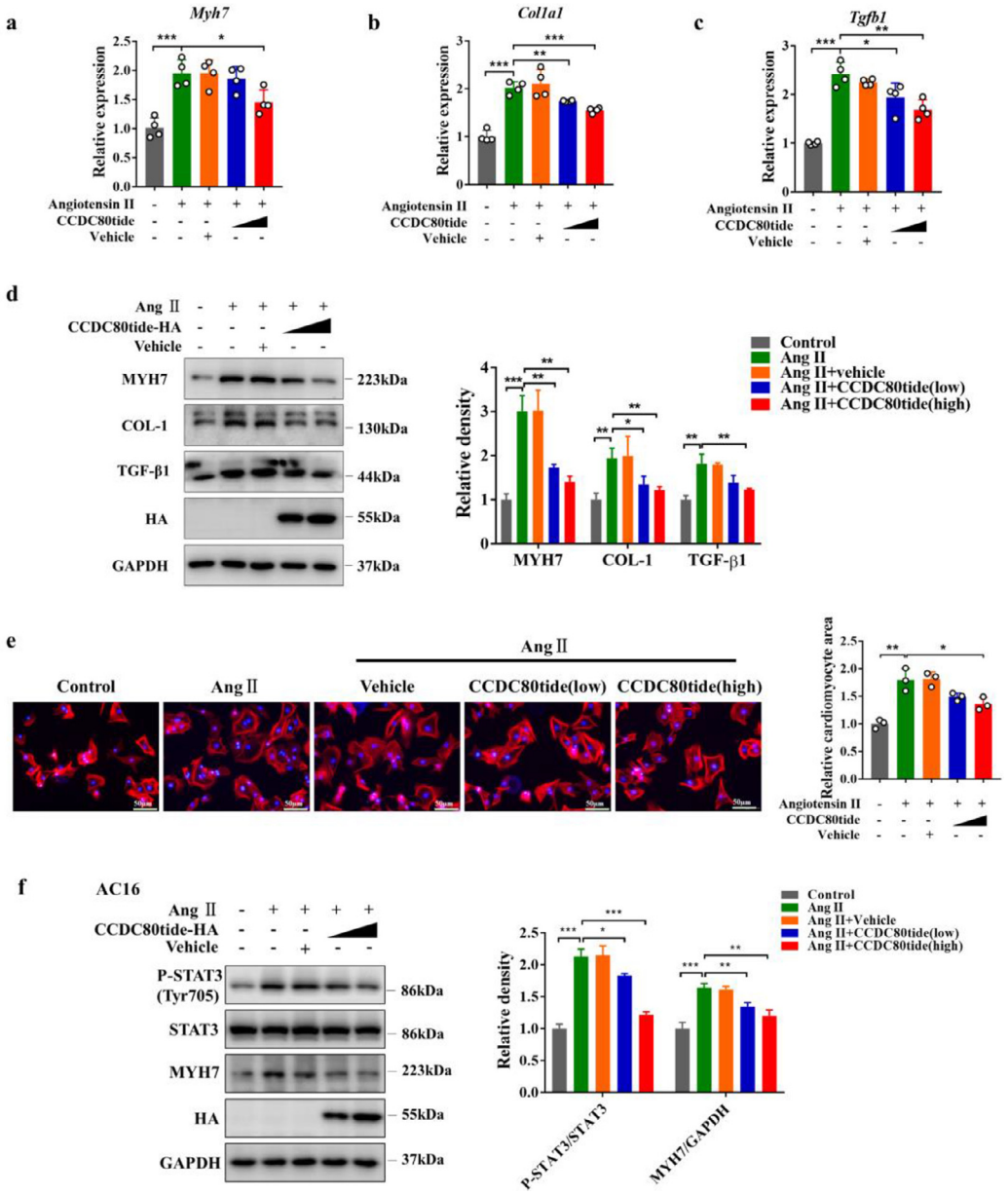

Figure 5. CCDC80tide ameliorates Ang II-induced hypertrophy in cultured cardiomyocytes.

a, b, c. Rat neonatal primary cardiomyocytes were infected with increasing levels of CCDC80tide-overexpressed lentivirus or empty lentivirus for 36 h, followed by 1-μM Ang II treatment for 6 h. Total RNA was extracted for qPCR analysis of *Myh7* (a), *Col1a1* (b), and *Tgfb1* (c) mRNA levels. The results are a representative of four biological repetitions.

d. Left panel, primary cardiomyocytes were infected with indicated lentivirus for 36 h and treated with 1 μM Ang II for 24 h. The total proteins were extracted and subjected to analysis of above mentioned three protein levels by WB. Right panel, densitometric quantification of WB. *N*=3

e. Left panel, representative images showing cultured primary cardiomyocytes stained with rhodamine phalloidin. Right panel, quantification of cardiomyocyte area. The results are representative of three biological repetitions (approximately 100 cells were randomly selected for calculation of mean value in each biological replicate, the same as below).

f. Left panel, AC16 cells were infected with increasing levels of CCDC80tide-overexpressed lentivirus or empty lentivirus for 36 h, followed by 1-μM Ang II treatment for 24 h. The total proteins were extracted and subjected to analysis of indicated protein levels by WB. Right panel, densitometric quantification of WB. *N*=3

Data are presented as mean ± SD. Statistical significance was determined using one-way ANOVA with Tukey's post hoc test. $^{*}p < 0.05$, $^{**}p < 0.01$, $^{***}p < 0.001$.

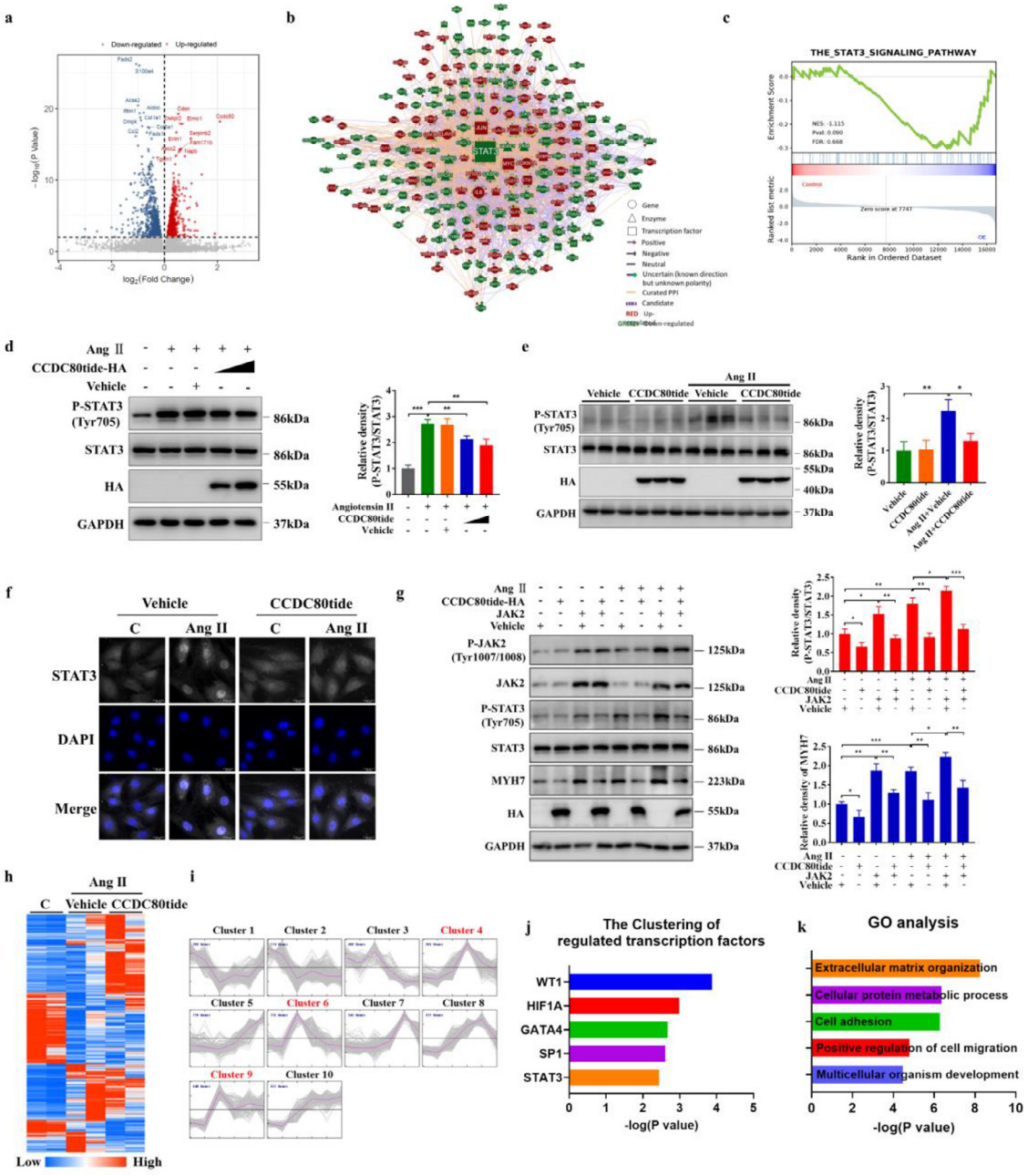

Figure 6. CCDC80tide ameliorated Ang II-induced hypertrophy through the regulation of STAT3 signaling.

Rat neonatal primary cardiomyocytes were infected with CCDC80tide-overexpressed lentivirus or empty lentivirus for 12 h; then, total RNA was extracted and subjected for RNA-seq analysis. Three biological replicates were used for RNA-seq analysis.

a. Volcano plot representing significant DEGs, $p < 0.01$ (CCDC80tide-overexpression group versus vehicle-overexpression group, upregulated in red and downregulated in blue). The top 10 ranked genes were labeled.

b. Establishing DEG network using a text mining approach based on GenCLiP 3. Red, the upregulated genes. Green, downregulated genes.

c. GSEA showing negative correlation between CCDC80tide overexpression and STAT3 signaling pathway.

d. Left panel, primary cardiomyocytes were infected with CCDC80tide-overexpressed lentivirus or empty lentivirus for 36 h, followed by 1-μM Ang II treatment for 24 h. The total proteins were extracted and subjected to analysis of STAT3 and p-STAT3 (Tyr705) protein levels by WB. Right panel, densitometric quantification of WB.

e. Left panel, mice were treated as described in Figure 5. The heart tissue protein was collected for WB analysis of STAT3 and p-STAT3 (Tyr705). Right panel, densitometric quantification of WB.

Phosphorylation of STAT3 Try705 was used as a molecular marker to monitor STAT3 activity. Consistent with previous studies,[62] Ang II caused a time-dependent increase in STAT3 Try705 phosphorylation in primary cardiomyocytes, and this effect was partially reversed by the expression of CCDC80tide (Supplemental Figure 9, Figure 6d). To confirm the effect of CCDC80tide on STAT3 activity *in vivo*, the cardiac tissue lysates extracted from mice challenged with Ang II or infected with CCDC80tide AAV were subjected to WB analysis. Encouragingly, CCDC80tide robustly inhibited Ang II-provoked p-Try705 of STAT3 (Figure 6e). Immunocytofluorescence staining showed that STAT3 was distributed throughout the cytoplasm and nucleus in the vehicle-treated cells (Figure 6f). However, Ang II-treated cells showed a prominent nuclear distribution of STAT3, and this effect was reversed by CCDC80tide overexpression (Figure 6f). The above mentioned findings suggest that CCDC80tide inhibits STAT3 activation excited by Ang II.

To explore the role of STAT3 signaling in CCDC80tide function, cardiomyocytes were transfected with two different siRNAs targeting STAT3. Knockdown of STAT3 decreased the content of MYH7, and the level of MYH7 was associated with the efficiency of STAT3 depletion (Supplemental Figure 10). Meanwhile, CCDC80tide has a potentiation effect on decreased STAT3 phosphorylation in STAT3 siRNAs-transfected cells, together with an enhanced inhibition on MYH7 in the presence of Ang II (Supplemental Figure 10). Of note, in the absence of Ang II, CCDC80tide did not reinforce the impact of STAT3 siRNA-2 on MYH7, in line with its little impact on p-STAT3 (Supplemental Figure 10, lane 3 and 9). To further prove CCDC80tide functions via JAK2/STAT3, we examined whether JAK2 overexpression could rescue CCDC80tide's effect (Figure 6g). As expected, JAK2 overexpression increases JAK2 phosphorylation, combined with elevated STAT3 phosphorylation. Under Ang II treatment, JAK2 overexpression restores the decreased p-STAT3 content caused by CCDC80tide overexpression, concomitantly with the recovery of MYH7 amount (lane 6 and 8).

To confirm the CCDC80tide/JAK2/STAT3 axis in vivo, RNA-seq was performed on mouse heart tissues after *in vivo* cardiac CCDC80tide overexpression. Dramatically, Ang II leads to a substantial transcriptome change while CCDC80tide treatment partially reverses it (Figure 6h). To further characterize the dynamic changes of gene expressions at the global level, we grouped differentially expressed genes (DEGs) into ten clusters using k-Means Clustering (KMC) (Figure 6i). The DEGs (Clusters 4, 6, and 9), whose expressions increase under Ang II treatment and decreased upon CCDC80tide overexpression, should be the key players regulated by CCDC80tide. Interestingly, transcriptional regulatory relationships of these DEGs are analyzed using the TRRUST website and reveal that STAT3 is one of the top enriched transcription factors (Figure 6j). Further GO analysis of these DEGs shows that extracellular matrix organization is the most significantly enriched biological process, which is the crucial molecular and cellular base of myocardial fibrosis (Figure 6k). Taken together, these data suggested that CCDC80tide ameliorated Ang II-induced hypertrophy through the regulation of STAT3 signaling.

CCDC80tide interacts with JAK2 and suppresses Ang II-induced activation of STAT3 signaling pathway

We then proceeded to elucidate the molecular mechanism by which CCDC80tide inhibits STAT3 signaling. A previous study demonstrated that CCDC80 is a binding partner for JAK2, the upstream signaling protein known to activate STAT3.[48] Given that CCDC80tide preserved more than half the structure of CCDC80, we speculated if CCDC80tide could interact with JAK2 and suppress its kinase activity. When 293T cells were co-transfected with CCDC80tide-HA and JAK2-Flag, IP of CCDC80tide-HA results in a clear coprecipitation of JAK2-Flag (Figure 7a). Similarly, JAK2-Flag could also precipitate CCDC80tide-HA (Figure 7b). JAK2 kinase activity is dependent on Try1007/1008 phosphorylation, which can be blocked by the catalytically mutation (K882E).[63] To examine whether JAK2 Try1007/1008

f. H9c2 cells were infected with CCDC80tide-overexpressed lentivirus or empty lentivirus for 36 h and then treated with 1 μM Ang II for 2 h. The nuclear translocation of STAT3 was examined by immunofluorescence staining using STAT3 antibody.

g. Left panel, H9c2 cells were infected with CCDC80tide-overexpressed lentivirus or empty lentivirus or JAK2-overexpressed lentivirus as indicated for 36 h and then treated with 1 μM Ang II for 24 h. The total proteins were extracted and subjected to analysis of indicated protein levels by WB. Right panel, densitometric quantification of WB.

h. Experimental condition is the same as that of Figure 4. After the experiment, RNA-seq is performed on mouse heart tissues. The heatmap displays differentially expressed genes with p value < 0.05.

i. To characterize the dynamic changes of gene expressions at the global level, differentially expressed genes (DEGs) were grouped into ten clusters using k-Means Clustering (KMC).

j. The DEGs (Clusters 4, 6, and 9) were subjected for analysis of transcriptional regulatory relationships using Transcription Factor Database TRRUST. The top 5 transcriptional factors (ranked by p -values) are shown.

k. The DEGs (Clusters 4, 6, and 9) were subjected for GO analysis. The top 5 transcriptional factors (ranked by p -values) are presented.

Data in D, E, F and G are mean ± SD; $n = 3$. P-values were determined by one-way ANOVA with Tukey's post hoc test.

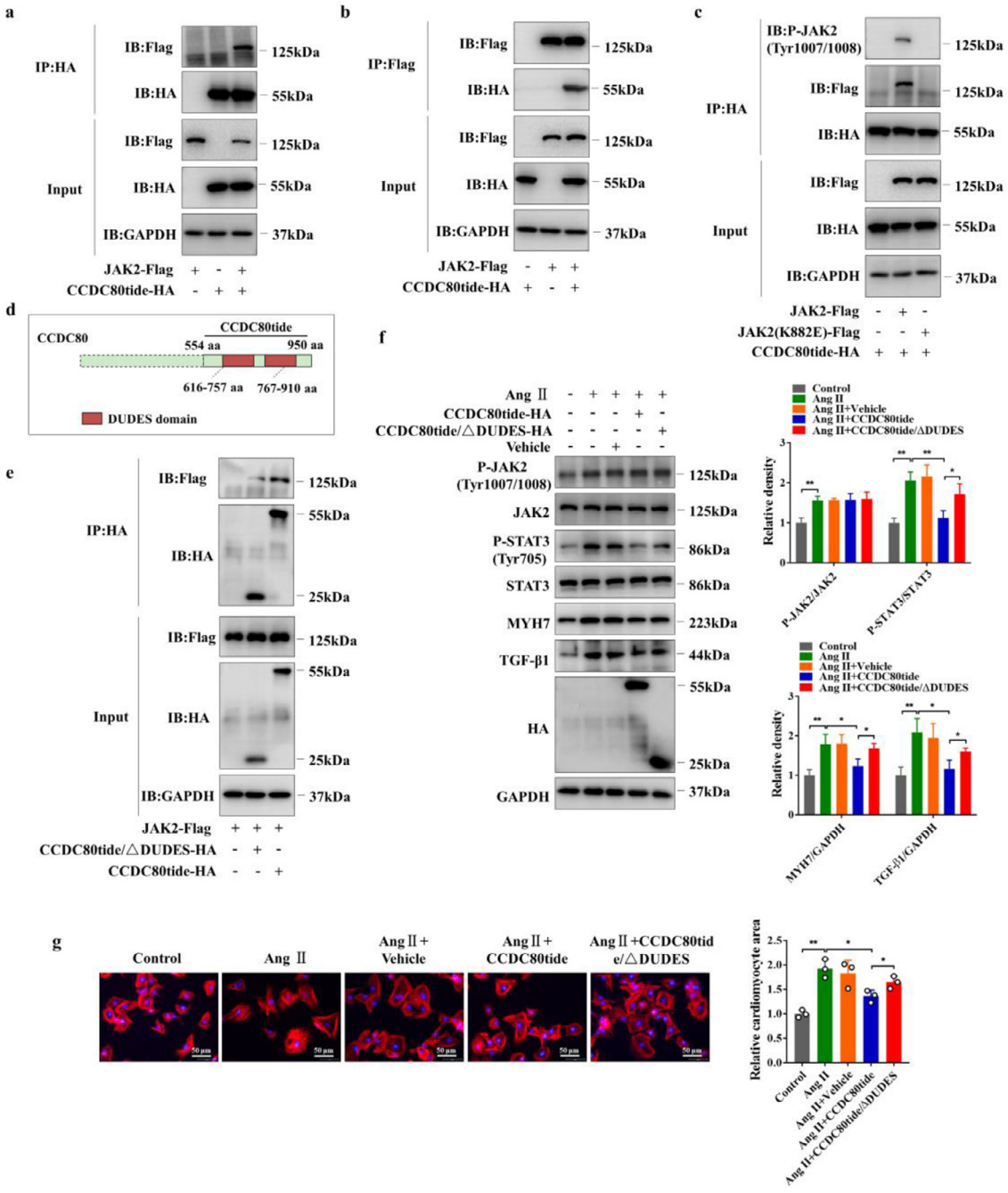

Figure 7. CCDC80tide interacts with kinase-active JAK2 dependent on DUDES domain.

a, b. 293T cells were co-transfected with HA-tagged CCDC80tide and Flag-tagged JAK2. Cell lysates were collected 48 h after transfection and immunoprecipitated with anti-HA magnetic beads (a) or anti-Flag agarose beads (b). The immunoprecipitates were probed by WB.

c. 293T cells were co-transfected with HA-tagged CCDC80tide and Flag-tagged JAK2 or catalytically inactive JAK2 (K882E). Cell lysates were collected 48 h after transfection and immunoprecipitated with anti-HA magnetic beads and analyzed by WB.

d. Schematic diagram of the DUDES domains of CCDC80tide.

e. 293T cells were co-transfected with Flag-tagged JAK2 and HA-tagged CCDC80tide or DUDES domain-deleted CCDC80tide (CCDC80tide/△DUDES). Cell lysates were collected 48 h after transfection and immunoprecipitated with anti-HA magnetic beads and analyzed by WB.

phosphorylation is required for JAK2 and CCDC80tide interaction, CCDC80tide-HA was co-transfected with either JAK2-Flag or JAK2 (K882E)-Flag. IP of CCDC80tide-HA resulted in coprecipitation of JAK2-Flag but not JAK2 (K882E)-Flag (Figure 7c). Moreover, the Try1007/1008 phosphorylation could be detected in precipitated JAK2 (Figure 7c), suggesting that the interaction of CCDC80tide and JAK2 is dependent on JAK2 Try1007/1008 phosphorylation.

Sequence analysis revealed that CCDC80tide contained two highly conserved domains: DRO1-URB-DRS-Equarin-SRPUL(DUDES) domains (616-757 aa, 767-910 aa) (Figure 7d). To determine whether DUDES domain is required for the interaction between CCDC80tide and JAK2, HA-tagged WT CCDC80tide or DUDES domain (616-757 aa)-depleted CCDC80tide (CCDC80tide/△DUDES-HA) was co-transfected with JAK2-Flag and then precipitated using anti-HA magnetic beads. The results showed that deletion of DUDES domain apparently reduced the interaction of JAK2 and CCDC80 (Figure 7e). The residual ability of CCDC80tide/△DUDES to bind JAK2 may be due to the remaining DUDES domain.

To investigate the contribution of JAK2 in CCDC80tide-afforded cardioprotection, the cardiomyocytes were overexpressed with CCDC80tide-HA or CCDC80tide/△DUDES-HA and then exposed to Ang II. Interestingly, the overexpression of CCDC80tide/△DUDES reduced STAT3 activation, coupled with the levels of myocardial hypertrophy and fibrosis markers (MYH7, TGF-β), to a less extent than CCDC80tide, although the expression of the mutant form was at a comparable level with that of intact form (Figure 7f). However, both of the two constructs had no effect on JAK2 activation induced by Ang II (Figure 7f). Furthermore, CCDC80tide/△DUDES exhibited a reduced ability to reverse cardiomyocyte hypertrophy compared with that of intact CCDC80tide (Figure 7g). These data suggest that the interaction between CCDC80tide and JAK2 is essential for CCDC80tide conferred cardioprotection under Ang II pressure.

Discussion

Diverse mechanisms have been reported to implicate in the interplay between physical activity and cardiovascular system. However, the mechanisms underlying cardioprotective effects afforded by exercise, particularly in pathological cardiac remodeling, remain unclear. Our work reveals a mechanism of exercise conferred protection against hypertensive cardiac remodeling. We identified exercise-derived CCDC80tide as a new cardioprotective molecule that ameliorates Ang II-induced cardiac remodeling in mice. Furthermore, CCDC80tide interacts with JAK2 through the DUDES domain and restricts pro-remodeling JAK2/STAT3 signaling activity, which inhibits cardiomyocyte hypertrophy. Our study provides new insights into understanding the mechanism underlying exercise-afforded protection against pathological cardiac remodeling.

Multiple roles of STAT3 have been revealed in cardiovascular diseases. Evidence from cardiac-specific transgenic mice suggested that STAT3 activation protects against cardiac I/R injury by promoting cell proliferation and inhibiting apoptosis.[64] Moreover, mice with cardiac-specific deletion of STAT3 are more susceptible to inflammation-induced heart damage and age-related cardiac fibrosis.[31] In contrast, STAT3 activation (p-Tyr705) contributes to Ang II-induced cardiac fibrosis,[65] and inhibition of JAK2/STAT3 activation by S3I-201 or celastrol ameliorates intermittent hypoxia or Ang II-induced cardiac fibrosis and remodeling.[29,62] Consistently, our work showed that restriction of STAT3 activation ameliorates cardiac remodeling induced by Ang II. The discrepancy may probably be due to the important role of STAT3 in heart development and cardiomyogenesis, which could influence the cardiac development and function in transgenic mice. Another possible explanation is the dominant biological events that STAT3 trigger differed due to the distinct pathophysiological contexts. These findings indicate that targeting the pathologic activation of STAT3 may hold promise as a potentially effective approach in preventing hypertensive cardiac remodeling.

CCDC80 (also known as URB, DRO1, and SSG1) contains a putative N-terminal secretory signal peptide. Indeed, CCDC80 was reported to be secreted in diverse types of cells,[46–48] except for dermal papilla cells, which only possess intracellular CCDC80.[66] Interestingly, once CCDC80 is secreted, it could be cleaved into several fragments between 50 and 120 kDa.[47,50,67] The secreted form and cleaved fragments of CCDC80 differ as physiopathological conditions change.[68] Previous studies focused more on CCDC80 and its fragments as secreted naked proteins . The EV encapsulation of the CCDC80 fragment during exercise has not been well characterized. The secretion of CCDC80 may determine

f. Left panel, rat primary cardiomyocytes were infected with CCDC80tide-overexpressed lentivirus or CCDC80tide/△DUDES lentivirus for 36 h and then treated with 1 μM Ang II for 24 h. The total proteins were extracted and subjected to analysis of indicated protein levels by WB. Right panel, densitometric quantification of WB.

g. Left panel, representative images showing cultured primary cardiomyocytes stained with rhodamine phalloidin. Right panel, quantification of cardiomyocyte area. The results are a representative of three biological repetitions.

Data are represented as mean ± SD; Data in a, b, c, e, f and g $n = 3$. Data in f and g, p-values were determined by one-way ANOVA with Tukey's post hoc test (right panel in f and g).

its behavior patterns and targets. Extracellular CCDC80 may act as an adipokine[68] and influence Wnt/β-catenin signaling to stimulate adipogenesis.[67] Intracellular CCDC80 may target JAK2 and ERK signals.[48,69] Thus, CCDC80 secretion and action is complicated and more evidence is needed to clarify the underlying regulatory mechanisms. Notably, the secretion of CCDC80 fragments was abolished upon the addition of protease inhibitors, concomitantly with increased amount of the full-length CCDC80,[67] suggesting a cell surface-anchored or extracellular protease-dependent generation of CCDC80 fragment. However, the detail mechanism by which CCDC80tide is selectively generated and encapsulated into EVs needs to be further researched. Our present study suggested that CCDC80tide interacts with kinase-active JAK2 through DUDES domain and affects STAT3 activation, without influencing tyrosyl-phosphorylation of the JAK2. We are curious about the mechanism underlying this biological process. Surprisingly, the DUDES domain itself is sufficient to bind to the tyrosine kinase domain (JH1) of JAK2.[48] Therefore, we speculated that CCDC80tide-DUDES may exclusively bind to JAK2-JH1 that hampers p-JAK2 to activate STAT3. Given the importance of DUDES domain in this process, exploring whether DUDES domain alone is sufficient to inhibit STAT3 signaling and following fibrosis phenotypes is an interesting line of research for future work, and this would contribute to CCDC80tide optimization and increase the potential for drug discovery.

An interesting question arising from our study is "What is the physiological significance of exercise-induced CCDC80tide release?" Physical exercise is a critical physiological stress that increases blood pressure and hemodynamic stimuli (e.g., increased shear stress) that presents a challenge to the cardiovascular system. The cardiovascular system has evolved several mechanisms to adapt to these changes, such as elevated nitric oxide (NO) bioavailability to improve vascular function.[70] Notably, physiological cardiac hypertrophy occurs in response to exercise stress to improve cardiac function and promote full adaptation of contractility to increased wall stress, whereas pathological hypertrophy occurs with volume or pressure overload. Additionally, the type of hypertrophic stimuli and nature of the downstream signaling largely determine the fate of cardiac hypertrophy, toward physiological or pathological.[71] Therefore, CCDC80tide release during exercise may be an important mechanism to combat pathological hypertrophy that helps the heart adapt to the exercise stress.

The current study has several limitations. First, although our data indicate that the skeletal muscle may be a source of CCDC80tide during exercise, validation of the origin of circulating CCDC80tide requires further investigations using a trace peptide in vivo or employing a skeletal muscle-specific knockout mice. Second, due to a technological limitation of the modulation of CCDC80tide within EVs specifically, it is currently difficult to conduct *in vivo* loss-of-function studies on circulating EVs in exercise-initiated cardioprotection. Third, only the level of CCDC80tide in healthy people was assessed. Further investigations in patients with cardiovascular risk factors are needed to characterize CCDC80tide in pathological conditions. Finally, the role of CCDC80tide in chronic exercise has not been well clarified. Although the myokine profile and muscle proteome overlap between acute and chronic exercise, the exerkines in response to these two types of exercises are not completely consistent.[72,73] Our data suggest that the amount of CCDC80 in skeletal muscle is increased after 3 months of swimming exercise (Figure 1J). Meanwhile, the literature showed that CCDC80 transcription is enhanced after 12 weeks of training.[36] These data indicate that CCDC80tide may also respond to chronic exercise. However, more evidence is needed to support this point.

Hypertensive cardiac hypertrophy is the leading cause of cardiac remodeling and heart failure. However, treatment and prevention strategies are still limited. Peptides are highly selective, efficacious, and relatively safe and well tolerated.[74] Our study indicates that CCDC80tide may be a potential therapeutic agent for treating hypertensive cardiac remodeling. Combined with our findings and previous report,[48] our results show that the DUDEs domain can interact with JAK2 and may be sufficient to mimic the function of CCDC80tide. Thus, the translational significance of CCDC80tide should be examined, including identification of the core functional sequence and optimal peptide modifications, such as a penetrated peptide linked to increased cell uptake and a cardiac tissue-specific targeting peptide linked to increased specificity.

In summary, we identified exercise-derived exosomal CCDC80tide as a new cardioprotective molecule that ameliorates Ang II-induced cardiac pathological hypertrophy. Our findings provide new insights into exercise-related cardioprotection and offer a potential therapeutic target for hypertensive cardiac remodeling.

Contributors

Anwen Yin performed conceptualization, methodology, investigation and writing-original draft preparation. Ruosen Yuan participated in investigation, visualization, software and data curation. Qingqing Xiao, Ke Xu and Weifeng Zhang were responsible for software and data curation. Xia Wang, Xiaoxiao Yang and Wentao Yang and Lei Xu performed formal analysis and software. Zhe Sun contributed to instruction and manuscript correction. Bin Zhou contributed to instruction. Yi Li, Zhaohua Cai and Fei Zhuang performed bioinformation and data analysis. Linghong Shen and Ben He performed conceptualization, supervision and funding acquisition. Anwen Yin, Ruosen Yuan, and Qingqing Xiao have directly accessed and verified the underlying

data in all research articles. Anwen Yin, Ruosen Yuan, and Linghong Shen were responsible for the decision to submit the manuscript. All authors read and approved the final version of the manuscript.

Data sharing statement

The data underlying this article are available in the article and in its online supplementary material. The data will be shared on reasonable request to the corresponding author.

Declaration of interests

None declared.

Acknowledgments

This work was supported by the National Natural Science Foundation of China [Grant/Award Numbers: 81770428, 81830010, 82130012, 81900438, 82100447); Shanghai Science and Technology Committee [Grant/Award Numbers: 21S11903000, 19JC1415702]; Emerging and Advanced Technology Programs of Hospital Development Center of Shanghai [Grant/Award Number: SHDC12018129]; China Postdoctoral Science Foundation [2021M692108]; and China National Postdoctoral Program for Innovative Talents [BX20200211].

Supplementary materials

Supplementary material associated with this article can be found in the online version at doi:10.1016/j.ebiom.2022.104164.

References

1 Ziaeian B, Fonarow GC. Epidemiology and aetiology of heart failure. *Nat Rev Cardiol*. 2016;13(6):368–378.
2 Metra M, Teerlink JR. Heart failure. *Lancet (London, England)*. 2017;390(10106):1981–1995.
3 Berk BC, Fujiwara K, Lehoux S. ECM remodeling in hypertensive heart disease. *J Clin Investigat*. 2007;117(3):568–575.
4 Drazner MH. The progression of hypertensive heart disease. *Circulation*. 2011;123(3):327–334.
5 Benjamin EJ, Muntner P, Alonso A, et al. Heart disease and stroke statistics-2019 update: a report from the American heart association. *Circulation*. 2019;139(10):e56–e528.
6 Wen CP, Wai JP, Tsai MK, et al. Minimum amount of physical activity for reduced mortality and extended life expectancy: a prospective cohort study. *Lancet (London, England)*. 2011;378(9798):1244–1253.
7 Penna C, Alloatti G, Crisafulli A. Mechanisms involved in cardioprotection induced by physical exercise. *Antioxidants Redox Sgnal*. 2020;32(15):1115–1134.
8 Bourdon A, Scott G, Keats A, et al. Aerobic exercise and cardiopulmonary fitness in childhood cancer survivors treated with a cardiotoxic agent: a meta-analysis. *Support Care Cance*. 2018;26(7):2113–2123.
9 Cavarretta E, Mastroiacovo G, Lupieri A, Frati G, Peruzzi M. The positive effects of exercise in chemotherapy-related cardiomyopathy. *Adv Experiment Med Biol*. 2017;1000:103–129.
10 Lavie CJ, Ozemek C, Carbone S, Katzmarzyk PT, Blair SN. Sedentary behavior, exercise, and cardiovascular health. *Circulat Res*. 2019;124(5):799–815.
11 Cattadori G, Segurini C, Picozzi A, Padeletti L, Anzà C. Exercise and heart failure: an update. *ESC Heart Failure*. 2018;5(2):222–232.
12 McMullen JR, Shioi T, Zhang L, et al. Phosphoinositide 3-kinase (p110alpha) plays a critical role for the induction of physiological, but not pathological, cardiac hypertrophy. *Proc Nat Acad Sci USA*. 2003;100(21):12355–12360.
13 Vega RB, Konhilas JP, Kelly DP, Leinwand LA. Molecular mechanisms underlying cardiac adaptation to exercise. *Cell Metabol*. 2017;25(5):1012–1026.
14 Liu X, Xiao J, Zhu H, et al. miR-222 is necessary for exercise-induced cardiac growth and protects against pathological cardiac remodeling. *Cell Metabol*. 2015;21(4):584–595.
15 Uchida S, Dimmeler S. Exercise controls non-coding RNAs. *Cell Metabol*. 2015;21(4):511–512.
16 Shi J, Bei Y, Kong X, et al. miR-17-3p contributes to exercise-induced cardiac growth and protects against myocardial ischemia-reperfusion injury. *Theranostics*. 2017;7(3):664–676.
17 Aoi W, Naito Y, Mizushima K, et al. The microRNA miR-696 regulates PGC-1{alpha} in mouse skeletal muscle in response to physical activity. *Am J Physiol Endocrinol Metabol*. 2010;298(4):E799–E806.
18 Gibb AA, Hill BG. Metabolic coordination of physiological and pathological cardiac remodeling. *Circulat Res*. 2018;123(1):107–128.
19 Schüttler D, Clauss S. Molecular mechanisms of cardiac remodeling and regeneration in physical exercise. *Cells*. 2019;8(10):1128.
20 Weiner RB, Baggish AL. Exercise-induced cardiac remodeling. *Prog Cardiovasc Dis*. 2012;54(5):380–386.
21 Pedersen BK, Febbraio MA. Muscles, exercise and obesity: skeletal muscle as a secretory organ. *Nature Rev Endocrinol*. 2012;8(8):457–465.
22 Safdar A, Saleem A, Tarnopolsky MA. The potential of endurance exercise-derived exosomes to treat metabolic diseases. *Nat Rev Endocrinol*. 2016;12(9):504–517.
23 Femminò S, Penna C, Margarita S, Comità S, Brizzi MF, Pagliaro P. Extracellular vesicles and cardiovascular system: biomarkers and cardioprotective effectors. *Vasc Pharmacol*. 2020;135:106790.
24 Frühbeis C, Helmig S, Tug S, Simon P, Krämer-Albers EM. Physical exercise induces rapid release of small extracellular vesicles into the circulation. *J Extracellular Vesicles*. 2015;4:28239.
25 Hou Z, Qin X, Hu Y, et al. Longterm exercise-derived exosomal miR-342-5p: a novel exerkine for cardioprotection. *Circulat Res*. 2019;124(9):1386–1400.
26 Chaturvedi P, Kalani A, Medina I, Familtseva A, Tyagi SC. Cardiosome mediated regulation of MMP9 in diabetic heart: role of mir29b and mir455 in exercise. *J Cellular Mol Med*. 2015;19(9):2153–2161.
27 Egan B, Zierath JR. Exercise metabolism and the molecular regulation of skeletal muscle adaptation. *Cell Metabol*. 2013;17(2):162–184.
28 Zhuang L, Jia K, Chen C, et al. DYRK1B-STAT3 drives cardiac hypertrophy and heart failure by impairing mitochondrial bioenergetics. *Circulation*. 2022;145(11):829–846.
29 Su SA, Yang D, Wu Y, et al. EphrinB2 regulates cardiac fibrosis through modulating the interaction of Stat3 and TGF-β/Smad3 signaling. *Circulat Res*. 2017;121(6):617–627.
30 Chen Y, Surinkaew S, Naud P, et al. JAK-STAT signalling and the atrial fibrillation promoting fibrotic substrate. *Cardiovasc Res*. 2017;113(3):310–320.
31 Jacoby JJ, Kalinowski A, Liu MG, et al. Cardiomyocyte-restricted knockout of STAT3 results in higher sensitivity to inflammation, cardiac fibrosis, and heart failure with advanced age. *Proc Nat Acad Sci USAm*. 2003;100(22):12929–12934.
32 Comità S, Femmino S, Thairi C, et al. Regulation of STAT3 and its role in cardioprotection by conditioning: focus on non-genomic roles targeting mitochondrial function. *Basic Res Cardiol*. 2021;116(1):56.
33 Heusch G, Musiolik J, Gedik N, Skyschally A. Mitochondrial STAT3 activation and cardioprotection by ischemic postconditioning in pigs with regional myocardial ischemia/reperfusion. *Circulat Res*. 2011;109(11):1302–1308.
34 Nan J, Hu H, Sun Y, et al. TNFR2 stimulation promotes mitochondrial fusion via Stat3- and NF-kB-dependent activation of OPA1 expression. *Circulat Res*. 2017;121(4):392–410.
35 Wu J, Guo W, Lin SZ, et al. Gp130-mediated STAT3 activation by S-propargyl-cysteine, an endogenous hydrogen sulfide initiator, prevents doxorubicin-induced cardiotoxicity. *Cell Death Dis*. 2016;7(8):e2339.

36 Pourteymour S, Eckardt K, Holen T, et al. Global mRNA sequencing of human skeletal muscle: Search for novel exercise-regulated myokines. *Mol Metabol*. 2017;6(4):352–365.
37 Rao RR, Long JZ, White JP, et al. Meteorin-like is a hormone that regulates immune-adipose interactions to increase beige fat thermogenesis. *Cell*. 2014;157(6):1279–1291.
38 Parker BL, Burchfield JG, Clayton D, et al. Multiplexed temporal quantification of the exercise-regulated plasma peptidome. *Mol Cellular Proteom*. 2017;16(12):2055–2068.
39 Forterre A, Jalabert A, Berger E, et al. Proteomic analysis of C2C12 myoblast and myotube exosome-like vesicles: a new paradigm for myoblast-myotube cross talk? *PLoS One*. 2014;9(1):e84153.
40 Kolur V, Vastrad BM, Tengli AR. Vastrad CM. Identification of candidate biomarkers and therapeutic agents for heart failure by bioinformatics analysis. *BMC Cardiovasc Disord*. 2021;21 (1):329.
41 Sasagawa S, Nishimura Y, Sawada H, et al. Comparative transcriptome analysis identifies CCDC80 as a novel gene associated with pulmonary arterial hypertension. *Front Pharmacol*. 2016;7:142.
42 Ramirez Flores RO, Lanzer JD, Holland CH, et al. Consensus transcriptional landscape of human end-stage heart failure. *J Am Heart Assoc*. 2021;10(7):e019667.
43 Lin J, Wu H, Tarr PT, et al. Transcriptional co-activator PGC-1 alpha drives the formation of slow-twitch muscle fibres. *Nature*. 2002;418(6899):797–801.
44 Akimoto T, Pohnert SC, Li P, et al. Exercise stimulates Pgc-1alpha transcription in skeletal muscle through activation of the p38 MAPK pathway. *J Biol Chem*. 2005;280(20):19587–19593.
45 Mathai AS, Bonen A, Benton CR, Robinson DL, Graham TE. Rapid exercise-induced changes in PGC-1alpha mRNA and protein in human skeletal muscle. *J Appl Physiol (Bethesda, Md: 1985)*. 2008;105(4):1098–1105.
46 Liu Y, Monticone M, Tonachini L, et al. URB expression in human bone marrow stromal cells and during mouse development. *Biochem Biophys Res Commun*. 2004;322(2):497–507.
47 Okada T, Nishizawa H, Kurata A, et al. URB is abundantly expressed in adipose tissue and dysregulated in obesity. *Biochem Biophys Res Commun*. 2008;367(2):370–376.
48 O'Leary EE, Mazurkiewicz-Muñoz AM, Argetsinger LS, Maures TJ, Huynh HT, Carter-Su C. Identification of steroid-sensitive gene-1/Ccdc80 as a JAK2-binding protein. *Mol Endocrinol (Baltimore, Md)*. 2013;27(4):619–634.
49 Misumi Y, Misumi Y, Miki K, Takatsuki A, Tamura G, Ikehara Y. Novel blockade by brefeldin A of intracellular transport of secretory proteins in cultured rat hepatocytes. *J Biol Chem*. 1986;261 (24):11398–11403.
50 Bommer GT, Jäger C, Dürr EM, et al. DRO1, a gene down-regulated by oncogenes, mediates growth inhibition in colon and pancreatic cancer cells. *J Biol Chem*. 2005;280(9):7962–7975.
51 Contrepois K, Wu S, Moneghetti KJ, et al. Molecular choreography of acute exercise. *Cell*. 2020;181(5):1112–1130.e16.
52 Pinto AR, Ilinykh A, Ivey MJ, et al. Revisiting cardiac cellular composition. *Circulat Res*. 2016;118(3):400–409.
53 Kivelä R, Hemanthakumar KA, Vaparanta K, et al. Endothelial cells regulate physiological cardiomyocyte growth via VEGFR2-mediated paracrine signaling. *Circulation*. 2019;139(22):2570–2584.
54 Granger DN, Kubes P. The microcirculation and inflammation: modulation of leukocyte-endothelial cell adhesion. *J Leukocyte Biol*. 1994;55(5):662–675.
55 Montezano AC, Nguyen Dinh Cat A, Rios FJ, Touyz RM. Angiotensin II and vascular injury. *Curr Hypertension Reports*. 2014;16(6):431.
56 Xiang R, Chen J, Li S, et al. VSMC-specific deletion of FAM3A attenuated Ang II-promoted hypertension and cardiovascular hypertrophy. *Circulat Res*. 2020;126(12):1746–1759.
57 Huo KG, Richer C, Berillo O, et al. miR-431-5p knockdown protects against angiotensin II-induced hypertension and vascular injury. *Hypertension (Dallas, Tex: 1979)*. 2019;73(5):1007–1017.
58 Schneider M, Kostin S, Strøm CC, et al. S100A4 is upregulated in injured myocardium and promotes growth and survival of cardiac myocytes. *Cardiovasc Res*. 2007;75(1):40–50.
59 Tamaki Y, Iwanaga Y, Niizuma S, et al. Metastasis-associated protein, S100A4 mediates cardiac fibrosis potentially through the modulation of p53 in cardiac fibroblasts. *J Mol Cellular Cardiol*. 2013;57:72–81.
60 Haghikia A, Stapel B, Hoch M, Hilfiker-Kleiner D. STAT3 and cardiac remodeling. *Heart Failure Reviews*. 2011;16(1):35–47.
61 Mascareno E, Siddiqui MA. The role of Jak/STAT signaling in heart tissue renin-angiotensin system. *Mol Cellular Biochem*. 2000;212(1-2):171–175.
62 Ye S, Luo W, Khan ZA, et al. Celastrol attenuates angiotensin II-induced cardiac remodeling by targeting STAT3. *Circulat Res*. 2020;126(8):1007–1023.
63 Watling D, Guschin D, Müller M, et al. Complementation by the protein tyrosine kinase JAK2 of a mutant cell line defective in the interferon-gamma signal transduction pathway. *Nature*. 1993;366 (6451):166–170.
64 Oshima Y, Fujio Y, Nakanishi T, et al. STAT3 mediates cardioprotection against ischemia/reperfusion injury through metallothionein induction in the heart. *Cardiovasc Res*. 2005;65 (2):428–435.
65 Bao Q, Zhang B, Suo Y, et al. Intermittent hypoxia mediated by TSP1 dependent on STAT3 induces cardiac fibroblast activation and cardiac fibrosis. *eLife*. 2020;9:e49923.
66 Cha SY, Sung YK, Im S, Kwack MH, Kim MK, Kim JC. URB expression in human dermal papilla cells. *J Dermatol Sci*. 2005;39 (2):128–130.
67 Tremblay F, Revett T, Huard C, et al. Bidirectional modulation of adipogenesis by the secreted protein Ccdc80/DRO1/URB. *J Biol Chem*. 2009;284(12):8136–8147.
68 Osorio-Conles O, Guitart M, Moreno-Navarrete JM, et al. Adipose tissue and serum CCDC80 in obesity and its association with related metabolic disease. *Molecular Medicine (Cambridge, Mass)*. 2017;23:225–234.
69 Gong D, Zhang Q, Chen LY, et al. Coiled-coil domain-containing 80 accelerates atherosclerosis development through decreasing lipoprotein lipase expression via ERK1/2 phosphorylation and TET2 expression. *Eur J Pharmacol*. 2019;843:177–189.
70 Hambrecht R, Adams V, Erbs S, et al. Regular physical activity improves endothelial function in patients with coronary artery disease by increasing phosphorylation of endothelial nitric oxide synthase. *Circulation*. 2003;107(25):3152–3158.
71 Nakamura M, Sadoshima J. Mechanisms of physiological and pathological cardiac hypertrophy. *Nat Rev Cardiol*. 2018;15 (7):387–407.
72 Little HC, Tan SY, Cali FM, et al. Multiplex quantification identifies novel exercise-regulated myokines/cytokines in plasma and in glycolytic and oxidative skeletal muscle. *Mol Cellular Proteomics*. 2018;17(8):1546–1563.
73 Petriz BA, Gomes CP, Almeida JA, et al. The effects of acute and chronic exercise on skeletal muscle proteome. *J Cellular Physiol*. 2017;232(2):257–269.
74 Fosgerau K, Hoffmann T. Peptide therapeutics: current status and future directions. *Drug Discovery Today*. 2015;20(1):122–128.